Quantum Information Processing with Ultracold Atoms and Molecules in Optical Lattices

Mirta Rodríguez

Instituto de Estructura de la Materia

CSIC, Madrid SPAIN

Overview

I. Introduction
   i. QIP requires the preparation, manipulation and detection of quantum states
   ii. Neutral particles trapped in optical lattices
II. Manipulation of neutral atoms
   i. Trapping with magnetic and laser fields
   ii. Optical lattices
   iii. Long-range interactions
III. Quantum state engineering with time-dependent potentials
   i. Twin-Fock states for Heisenberg limited interferometry
   ii. Fast oscillatory potentials for scanning the phase diagram
   iii. Trains of pulses to align molecules
IV. Detection of strongly-correlated states of ultracold atoms
   i. Quantum Polarization Spectroscopy
   ii. Atom counting
V. Quantum gate operations in optical lattices
   i. Experimental realization of gate operations with atoms
   ii. QI with polar molecules: a theoretical proposal

I.
Introduction

1. Requirements for QIP
2. Hubbard-Hamiltonians with optical lattices

I. Requirements for QIP (DiVincenzo)

- Quantum register: set of qubits

  Superpositions & entanglement
- Isolated from environment → prevent decoherence
- Universal set of gates: two-qubit gate & single qubit operations
- Initial state preparation
- Detection of the quantum states
- Scalability of the system
- Networking ability

I. Requirements for QIP

➔ Quantum State Engineering

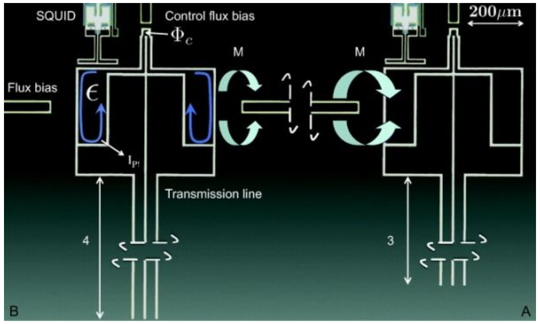

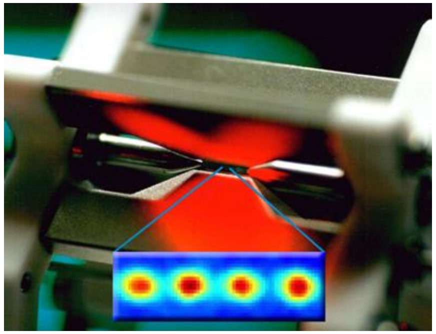

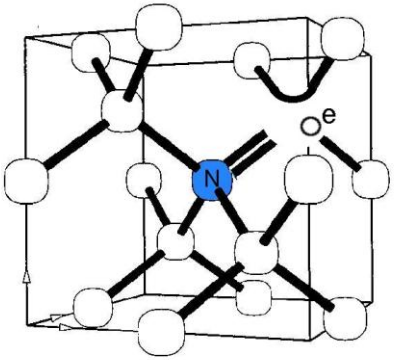

Candidates for QIP

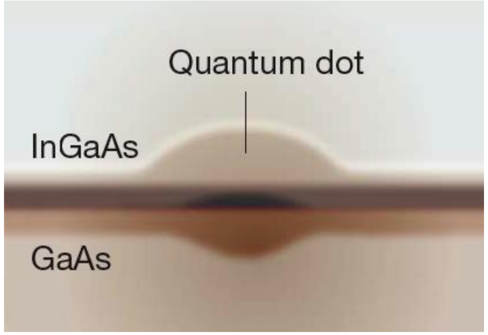

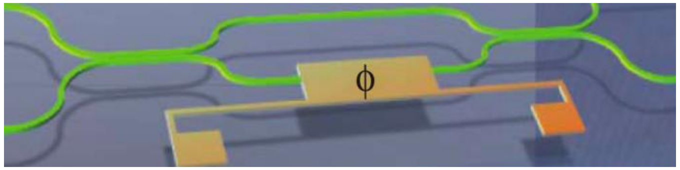

II. Neutral particles trapped in Optical Lattices

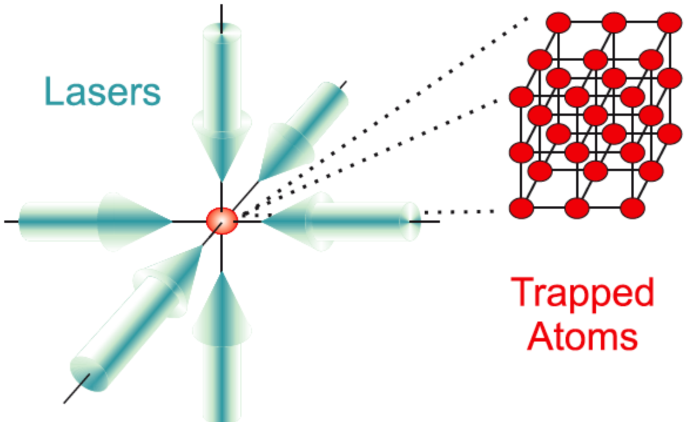

D. Jaksch, Contemporary Physics 2004

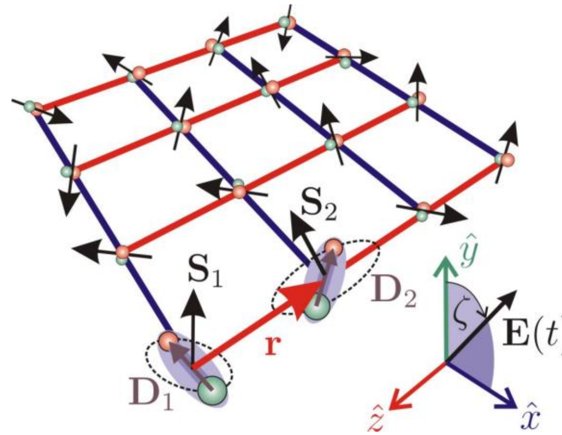

Zoller et al PRA 76,043604 (2007)

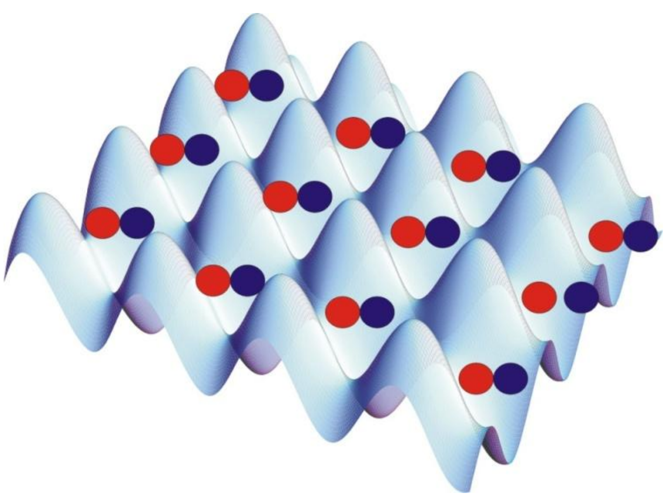

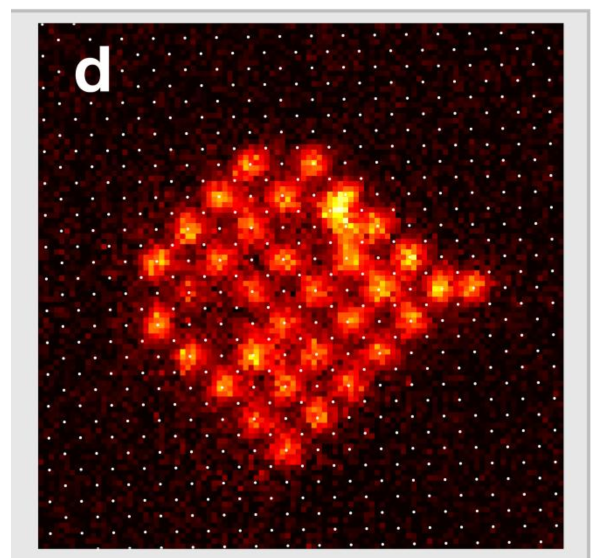

I. Bloch's group arxiv:1101.2076

Key elements

1) Qubits $\{|0\rangle_j, |1\rangle_j\}$

$$|\Psi\rangle = \sum_{j_1,j_2,\ldots j_N=0}^{1} c_{j_1 j_2 \ldots j_N} |j_1\rangle_1 \otimes |j_2\rangle_2 \otimes \ldots \otimes |j_N\rangle_N$$

2) Low decoherence rates: neutral particles with small dipole moments

3) Large systems

4) High controllability: engineering of Hamiltonians and strongly correlated quantum states

Engineering Hamiltonians

$$\boldsymbol{H} = \Sigma_{\boldsymbol{\sigma} jj'} \mathrm{T}_{\boldsymbol{\sigma} j}\, \boldsymbol{b}^{+}_{\sigma j} \boldsymbol{b}_{\sigma j'} + \Sigma_{\boldsymbol{\sigma} jk} \mathrm{U}_{\sigma\sigma' jk}\, \boldsymbol{b}^{+}_{\sigma j} \boldsymbol{b}^{+}_{\sigma' k} \boldsymbol{b}_{\sigma' k} \boldsymbol{b}_{\sigma j}$$

i) single and two-qubit interactions

ii) many-body quantum states are strongly correlated such that interactions between qubits of the same order as the single qubit energies

iii) many-body states are characterized by correlations $<b^{(+)}_{\sigma j} b_{\sigma' k}>$ which break the symmetries and define complicated phase diagrams characterized by $U_{\sigma\sigma'}/T_{\sigma}$.

quantum phase transitions

iv) strong correlations → entanglement

5) Entanglement

Strongly correlated phases in optical lattices

Challenges:

- On-site resolution is difficult as interparticle distance in the order of the diffraction limit of light.

  On-site manipulation & detection is now possible ✔
- Neutral particles with small dipole moments result only in on-site interactions in the lattice.

  Long-range interactions appear in ultracold molecules ✔

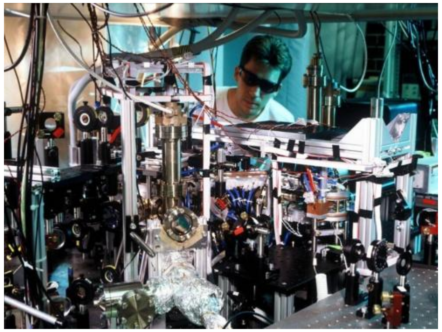

II.
Manipulation of neutral atoms

I. Ultracold samples are manipulated with magnetic and laser fields
II. Optical Lattice potentials
III. Long-range interactions

I. Ultracold atomic samples

- Quantum degenerate regime

  deBroglie wavelength $\lambda_T \sim (mT)^{-1/2} \sim$ interparticle distance $n^{-1/3}$

  gas samples are dilute ~10^{13-15} cm^{-3} and ultracold ~100nK

- Alkali atoms

  electronic spin J=L+S L=0 → J=1/2

  I nuclear spin

  total spin F=I+J → F=I±1/2

  I=3/2 for ^{87}Rb

  Total spin → Fermi/Bose statistics

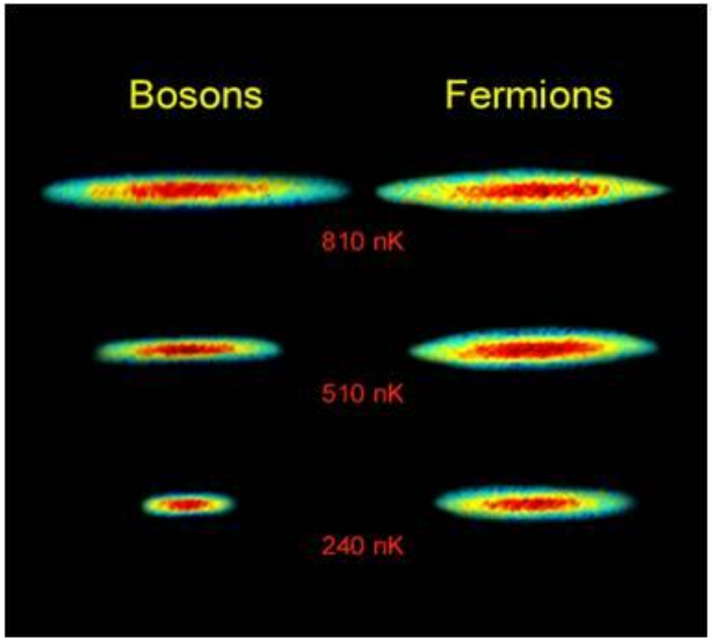

R. Hulet's group

- Dilute→ 2-body collisions whose sign

- Trapping with magnetic fields and opt

- Imaging with CCD camera

I. Magnetic and optical trapping

- Zeeman splitting

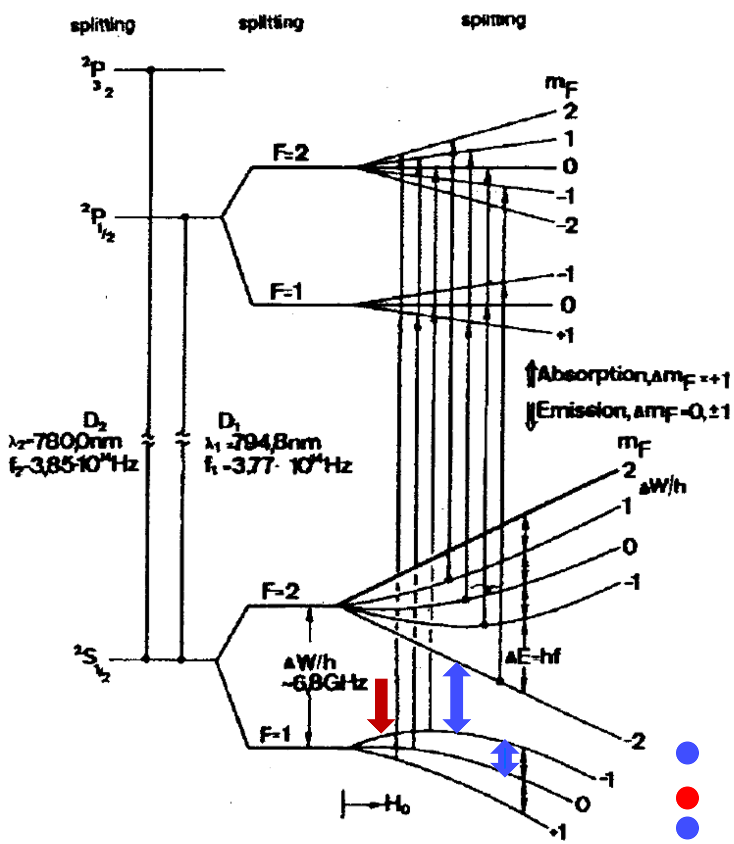

Fig. 1 Energy Level Scheme for Rb^{87}

- Optical dipole force

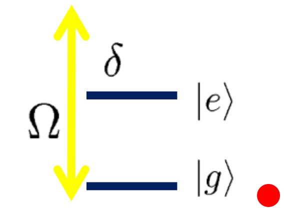

Interaction of atom with laser field

H_{int}=**-d E**=-d E(r)cos(ωt+ϕ)

If the laser is far detuned from the transition it remains in the ground state and experiences an effective dipole potential

$$V(\mathbf{r}) = \frac{\hbar\delta\Omega(\mathbf{r})^2}{\delta^2}$$

$$\Omega(\mathbf{r}) \ = \langle e|\mathbf{d}\cdot\hat{\mathbf{e}}E(\mathbf{r})e^{i\varphi(\mathbf{r})}|g\rangle/2$$

II. Optical lattice potentials

Counter-propagating laser beams result in a standing-wave configuration

$$V(r) \sim I = I_0 \cos^2(\mathbf{k} \cdot \mathbf{r})$$

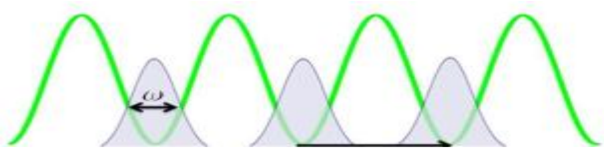

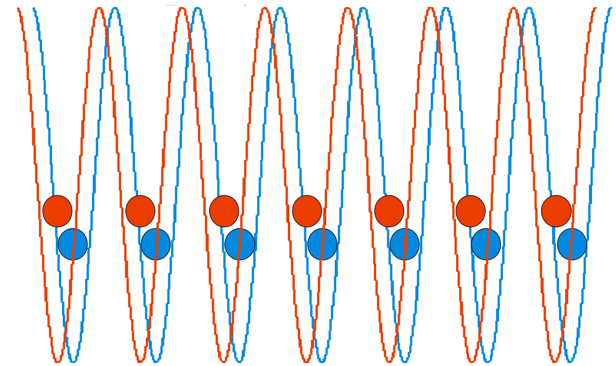

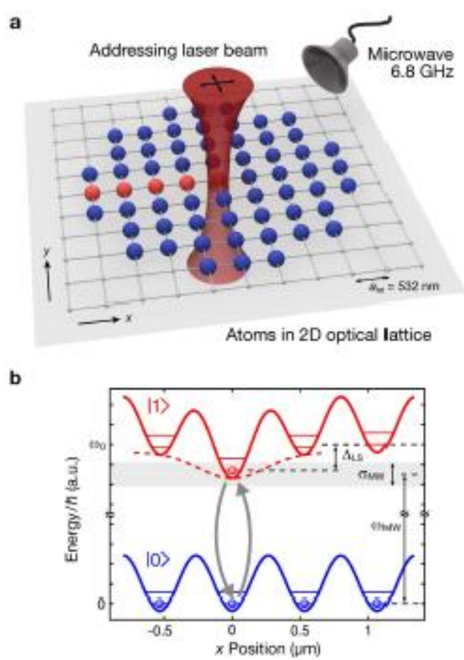

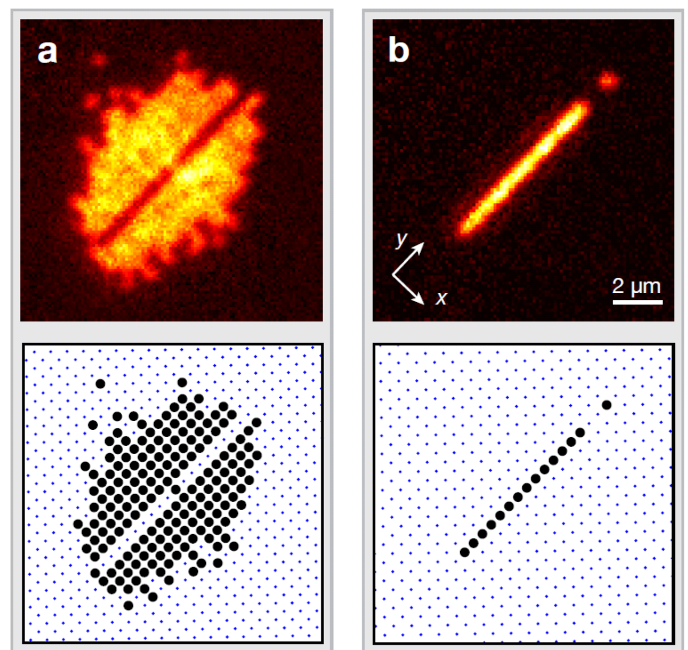

I. Bloch's group arxiv:1101.2076, Greiner's group Nature 2009

II. Hubbard model

tight-binding regime: kinetic energy+ two-body interactions

$$\hat{K} = \int d\mathbf{r} \sum_{\sigma=\uparrow,\downarrow} \left[\hat{\psi}^\dagger_\sigma(\mathbf{r}) \left(-\frac{\hbar^2\nabla^2}{2m} + V_\sigma(\mathbf{r}) - \mu_\sigma \right) \hat{\psi}_\sigma(\mathbf{r}) \right]$$
$$+\frac{1}{2} \sum_{\sigma,\beta=\uparrow,\downarrow} \int d\mathbf{r} \int d\mathbf{r}' u_{\sigma\beta}(\mathbf{r}-\mathbf{r}') \hat{\psi}^\dagger_\sigma(\mathbf{r}) \hat{\psi}^\dagger_\beta(\mathbf{r}') \hat{\psi}_\beta(\mathbf{r}') \hat{\psi}_\sigma(\mathbf{r}),$$

$$\hat{\psi}_\sigma(\mathbf{r}) = \sum_j \hat{c}_{j\sigma} w(\mathbf{r}-\mathbf{r_j})$$

$$\boxed{H_0 = J \sum_{\langle i,j \rangle \sigma} c^\dagger_{i\sigma} \hat{c}_{j\sigma} + U \sum_j c^\dagger_{j\uparrow} c^\dagger_{j\downarrow} \hat{c}_{j\downarrow} \hat{c}_{j\uparrow}}$$

$$J = -\int d\mathbf{r} w^\dagger(\mathbf{r}-\mathbf{r_i}) \left[-\frac{\hbar^2\nabla^2}{2m} \right] w(\mathbf{r}-\mathbf{r_j})$$

tunneling rate

$$U = \frac{4\pi a_s \hbar^2}{m} \int d\mathbf{r} |w(\mathbf{r})|^4$$

on-site two-body interaction

II. Superfluid to Mott-insulator transition: initialization of a qubit register

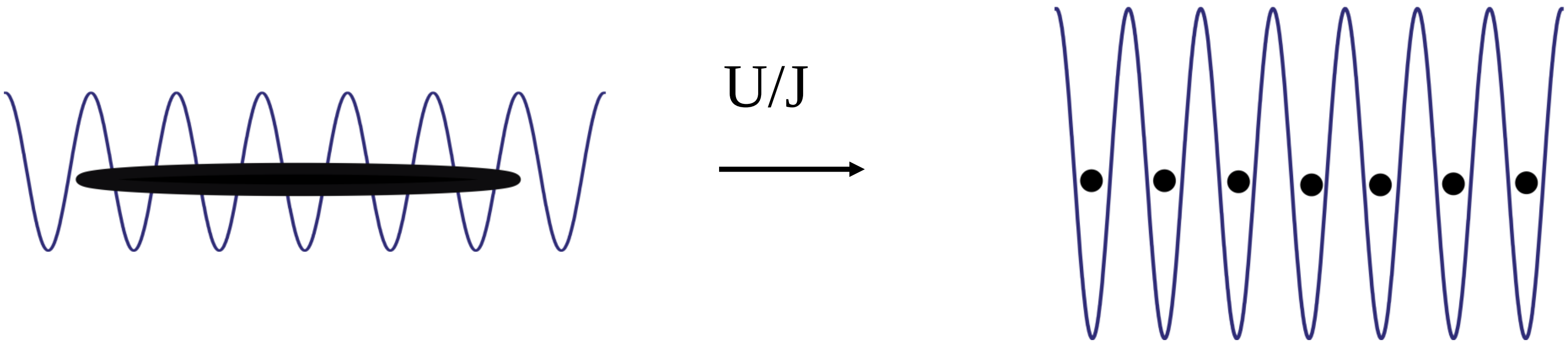

$$H = -J \sum_j \left(a_j^\dagger a_{j+1} + a_{j+1}^\dagger a_j \right) + \frac{U}{2} \sum_j n_j (n_j - 1)$$

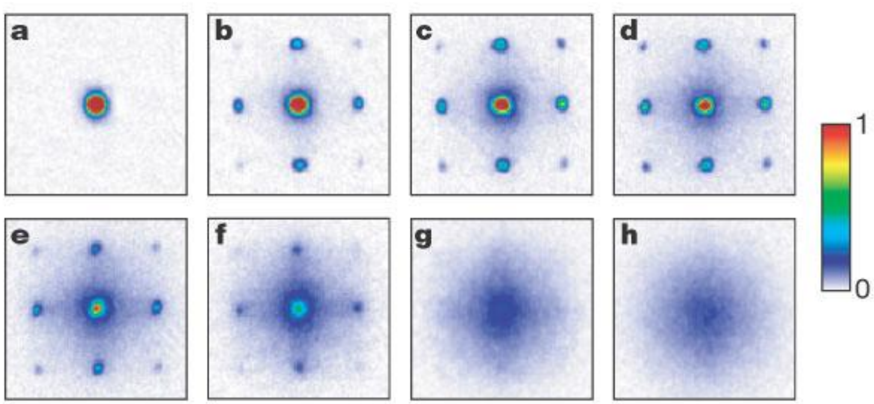

a-h $V_0 = 0\text{-}20\ E_R$

$$n \propto \sum_{i,j} e^{ik(r_i - r_j)} \langle a_i^\dagger a_j \rangle$$

D. Jaksch et al, PRL 81,3108 (1998)
Experiment:
M. Greiner, O. Mandel, T. Esslinger, T. W. Haensch and I. Bloch, Nature **415**, 39 (2002)

III. Long-range interactions in neutral atoms

- Strong magnetic moments: Chromium atoms

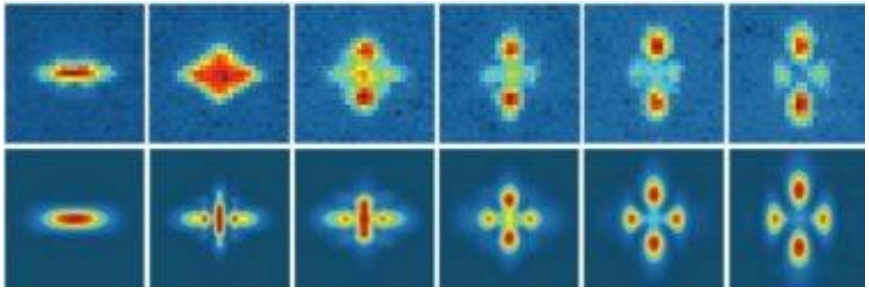

T. Pfau's group Stuttgart

- Cavity induced long-range interactions

- Coupling to Rydberg states of the atoms

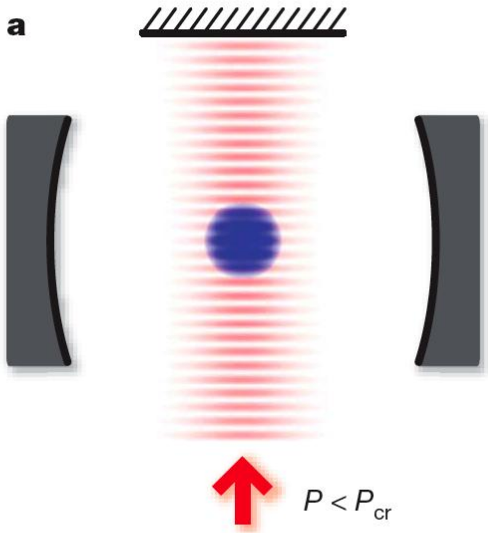

T. Esslinger's group Nature 464 (2010)

III. Dipolar molecules

- In the presence of external fields, molecules present high effective dipolar moments depending on the **rotational states** of the molecule.
- Strong electric dipole moments result in long-range dipole-dipole interactions between the molecules

$$H_{dd} = \frac{\mathbf{d}_1 \cdot \mathbf{d}_2 - 3(\mathbf{d}_1 \cdot \mathbf{e}_R)(\mathbf{e}_R \cdot \mathbf{d}_2)}{R^3}$$

- Hubbard-Hamiltonians with long-range interactions could be realized.

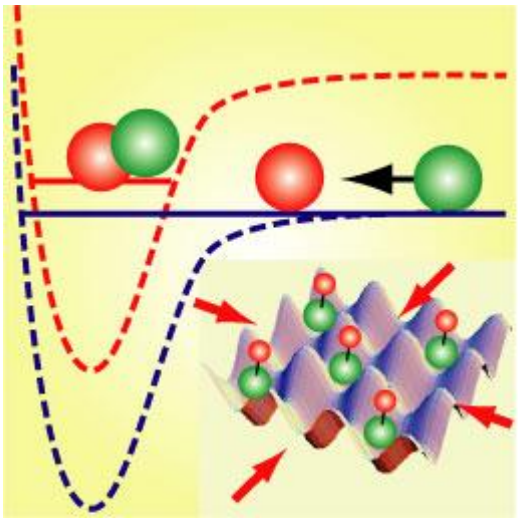

Experiments with dipolar dimers at JILA and Innsbruck are at the edge of reaching **quantum degeneracy** !!

PRA 76,043604 (2007)

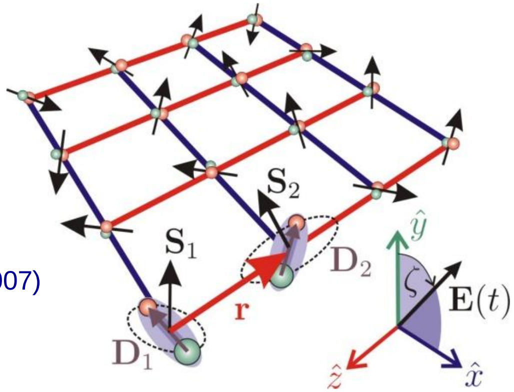

III.
Quantum state engineering with time dependent fields

I. Twin-Fock states for Heisenberg-limited interferometry
II. Fast oscillatory potentials to cross the phase diagram
III. Orientation of molecules with trains of laser pulses

III.I

Generation of twin-Fock states for Heisenberg-limited interferometry

Melting the state $$|\Psi_{ab}\rangle = \prod_{i=1}^{N} |ab\rangle_i$$

Two-component Mott insulators

- Components: ***hyperfine states*** of the atom
- MI regime → 2-body physics

Control of the spin interactions in an optical lattice

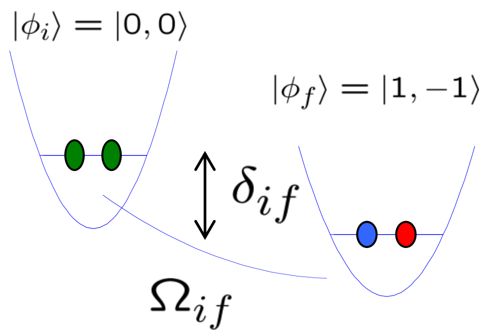

Rabi oscillations in 2-level system

$$P_{if} = \frac{\Omega'^2_{if}}{2\delta^2_{if}}(1 - \cos(\Omega'_{if} t))$$

$$\Omega_{if} = \sqrt{\Omega^2_{if} + \delta^2_{if}}$$

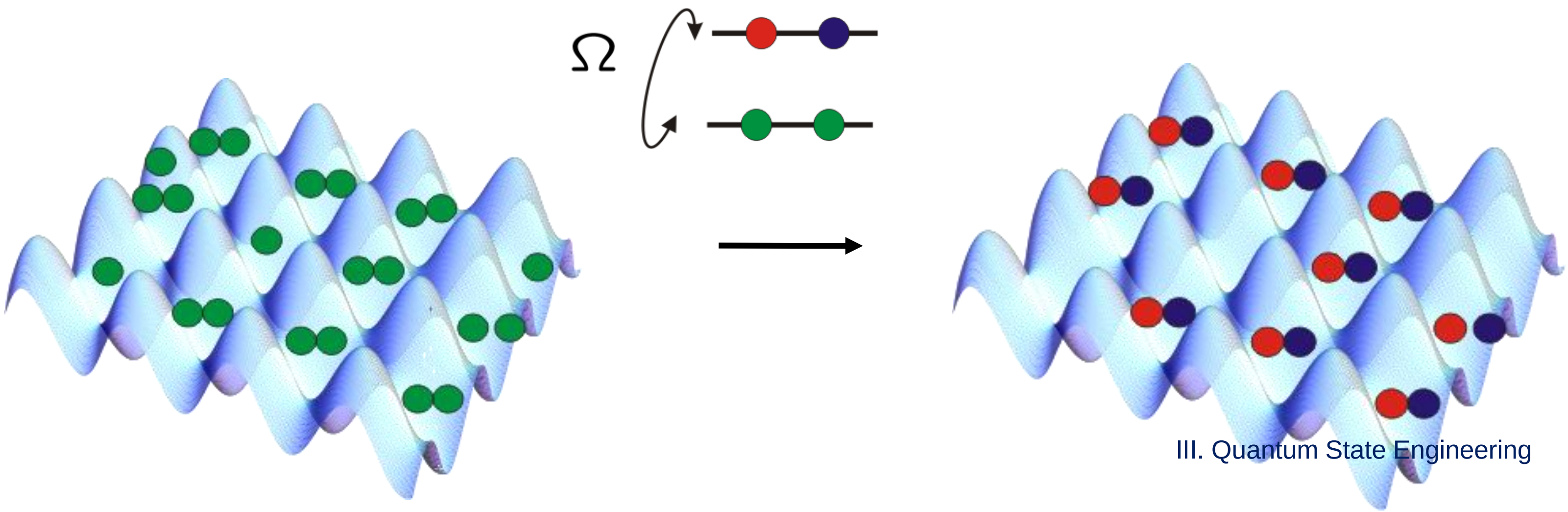

Bose-Hubbard Hamiltonian

$$H = -J \sum_{\langle i,j \rangle} (a_i^\dagger a_j + b_i^\dagger b_j) + U \sum_i n_i^a n_i^b + \sum_i \frac{V}{2} n_i^a (n_i^a - 1) + \sum_i \frac{V}{2} n_i^b (n_i^b - 1)$$

J tunneling rate

V intraspecies on-site interactions

U interspecies interactions

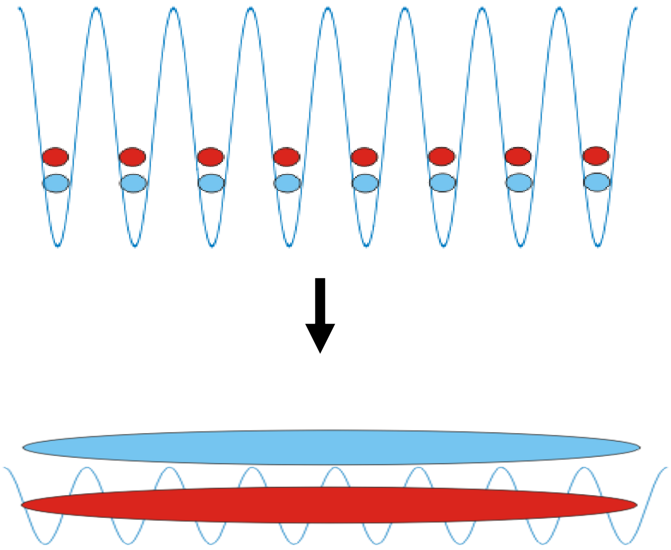

U/V fixed and $V/J \to 0$

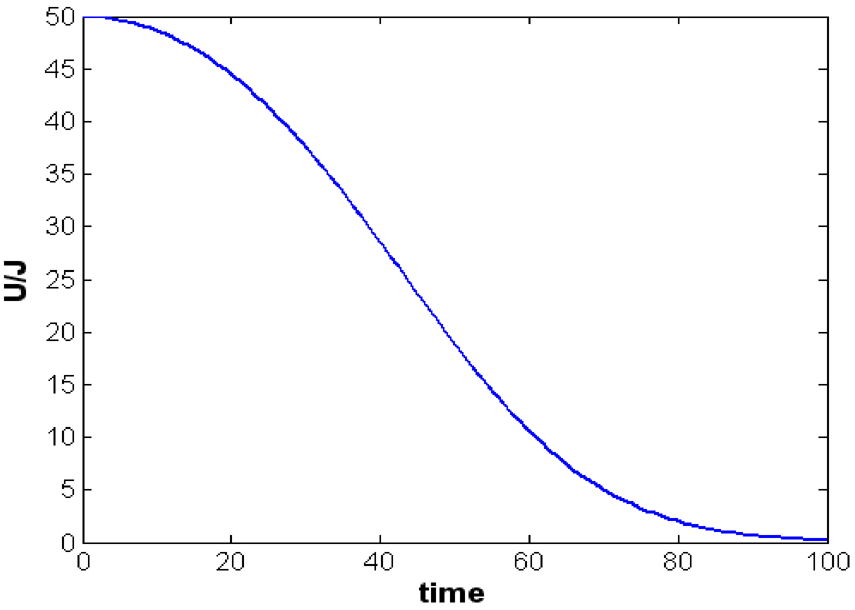

Adiabatic Evolution

- During adiabatic evolution the system follows the instantaneous eigenstates.
- **Non-crossing rule:** If the Hamiltonian depends only on one parameter λ, the energies of the states as a function of λ do not cross for states of the same symmetry.
- The curves approach each other at avoided crossings (Landau-Zener)

$$\langle\psi|H(\lambda)|\psi\rangle$$

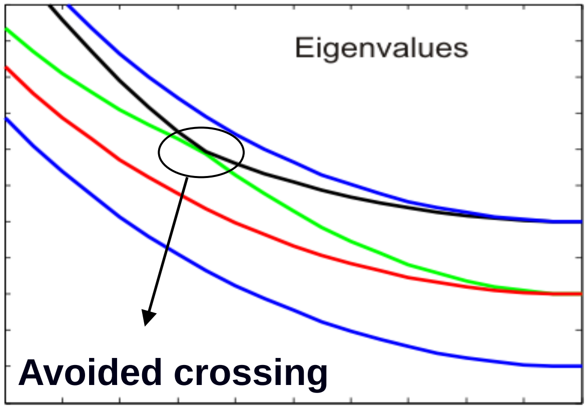

λ

Adiabatic evolution

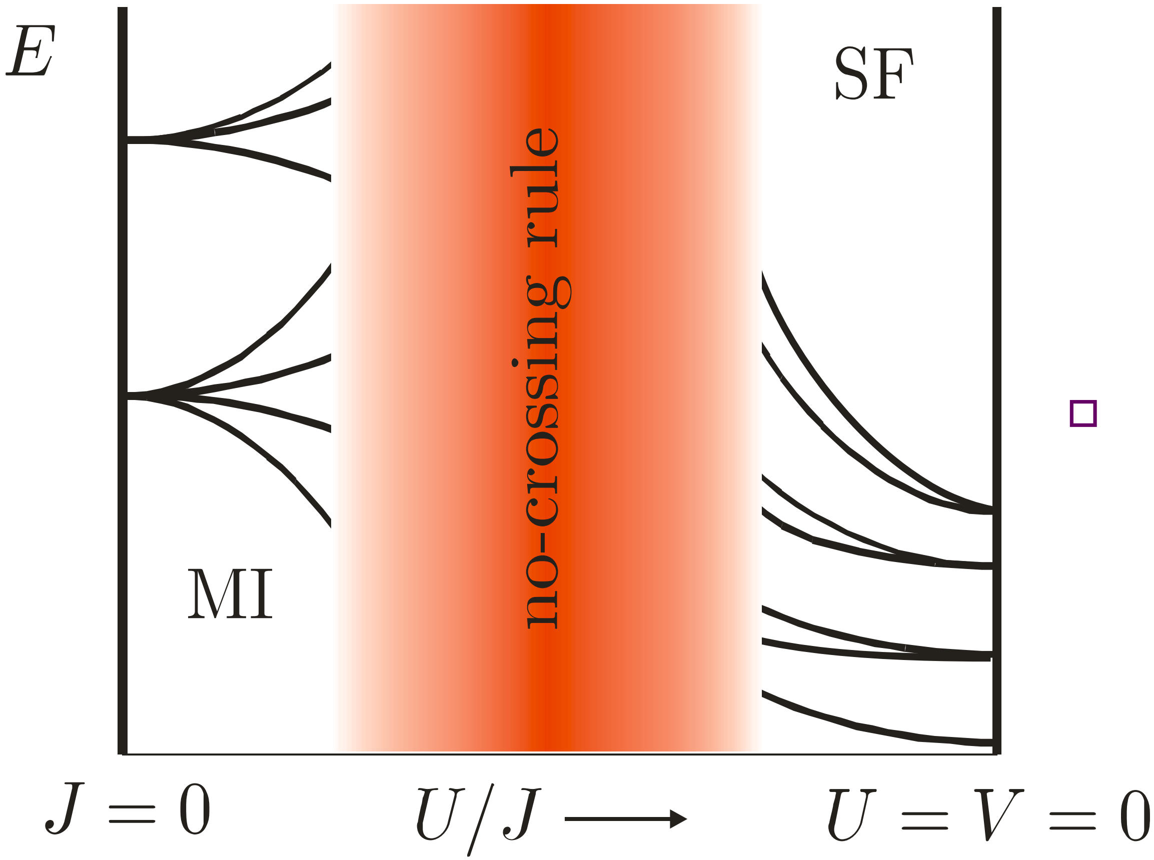

- We map initial superposition states into final superpositions with same coefficients with the dynamical phase

- Adiabatic time scale in a one-component system

$$Jt_r \gg \frac{VN}{JM}$$

It does not scale with N!

Twin-Fock state (I)

- **MI regime** (J→ 0) $|\Psi_{ab}\rangle = \prod_{i=1}^{N} |ab\rangle_i$

  Non-degenerate ground state if U < V

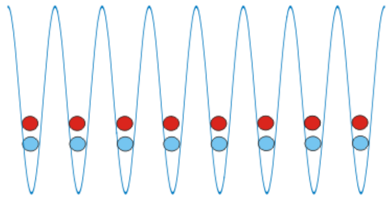

- **SF regime** (V→0) $|\Psi_{tf}\rangle = |N/2\rangle_{A_0} |N/2\rangle_{B_0}$

  The non-degenerate ground state for each mode is the delocalized symmetric state A_0,B_0

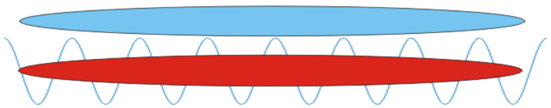

$A_0^\dagger \sim \sum_i a_i^\dagger$ $B_0^\dagger \sim \sum_i b_i^\dagger$

- The two non-degenerate ground states are connected by adiabatic evolution

Adiabatic melting $|\Psi_{ab}\rangle$ provides a direct means of obtaining a **twin-Fock state** with zero relative number.

This state useful in atom interferometric experiments!!!

Exact calculation for M=6 sites

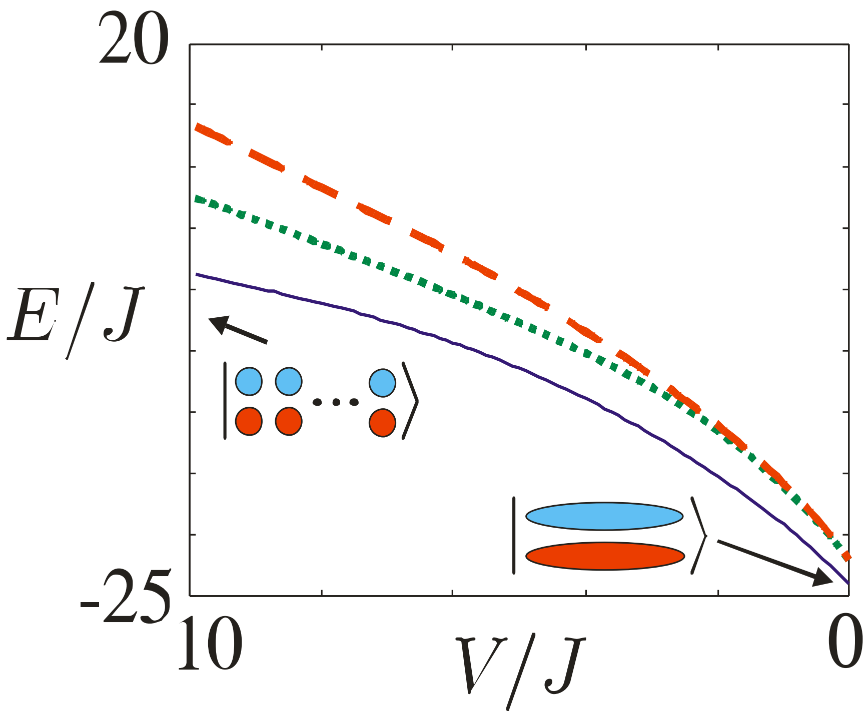

Spectrum of the 2 BHM in the symmetric subspace with $N_a=N_b=6$ and V/U=0.1.

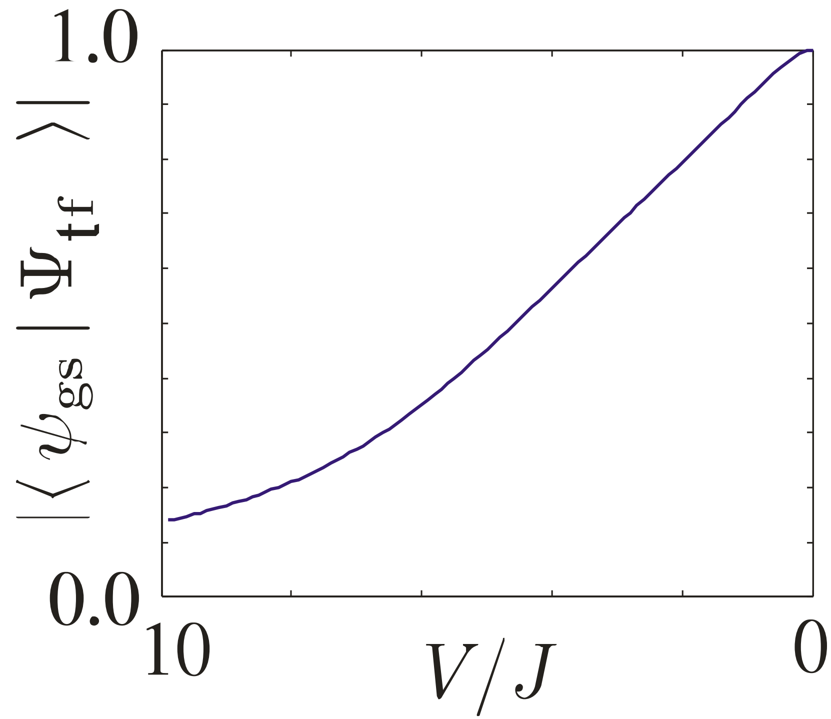

Overlap of the instantaneous ground state of the BHM and the twin-Fock state.

TEBD (t-DMRG) calculation

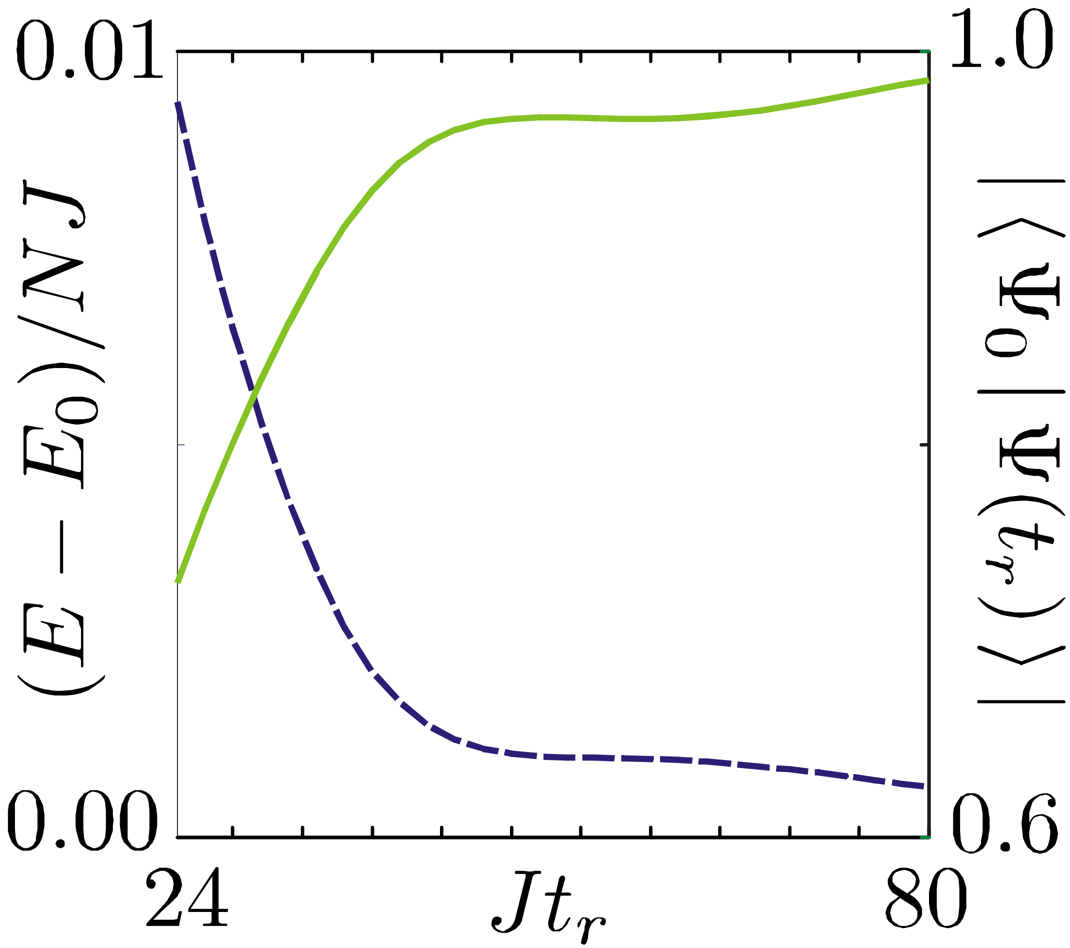

Energy difference per atom and overlap between the ramped state and the final SF ground state for different ramping times t_r. ($V_0/J=20$, $M=25=N_a=N_b$)

Adiabatic ramping time scale

$J\,t_r \sim 3\,V_0/J$

Large systems and interferometry

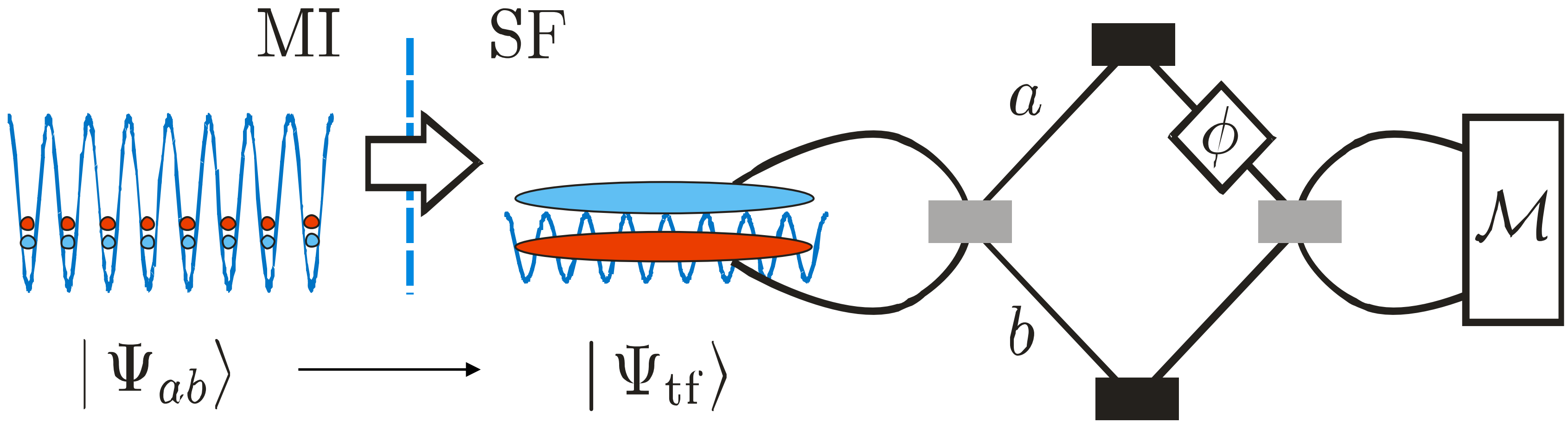

Objective: measure phase differences ϕ with highest sensitivity

Shot noise limit

$$\Delta\phi \sim N^{-1/2}$$

Heisenberg limit

$$\Delta\phi \sim N^{-1}$$

Sensitivity across the Mott insulator transition

$$\Delta\phi(0) = \frac{1}{2\sqrt{\langle J_x^2\rangle}}$$

$$\langle J_x^2\rangle = [\sum_i(\rho^a_{ii}+\rho^b_{ii}) + \sum_{i,j}(\rho^a_{ij}\rho^b_{ji} + \text{h.c.})]/4$$

$$\rho^a_{ij} = \langle a_i^\dagger a_j\rangle$$

$$\Delta\Phi \sim N^{-\alpha}$$

SF

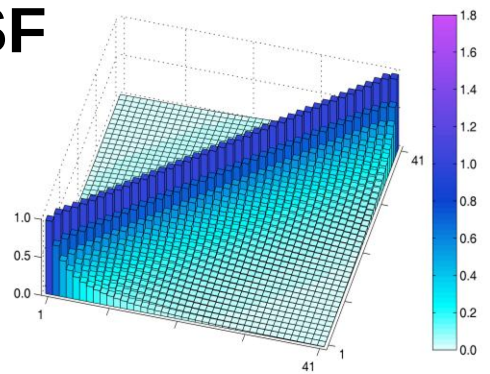

$\rho^{a,b}_{ij} = 1 \rightarrow \Delta\phi(0) = 1/\sqrt{N^2/2+N}$

$\Delta\phi \sim N^{-1}$ **Heisenberg limit**

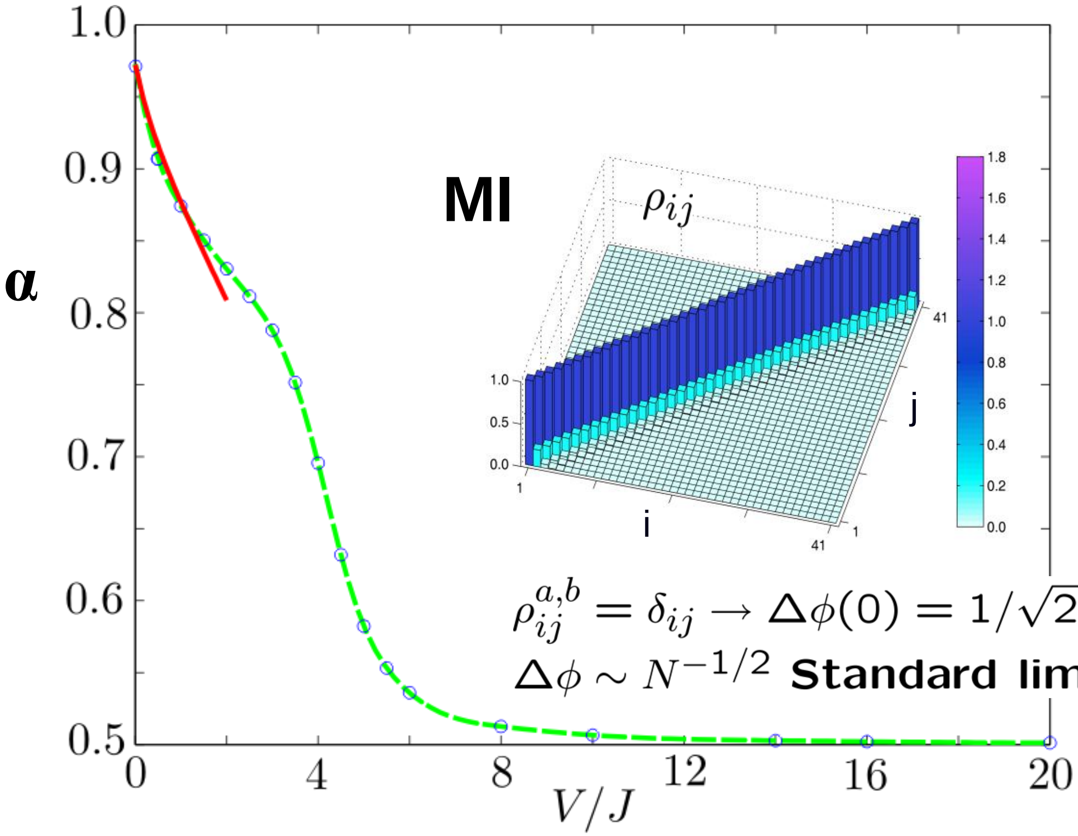

$\rho^{a,b}_{ij} = \delta_{ij} \rightarrow \Delta\phi(0) = 1/\sqrt{2N}$

$\Delta\phi \sim N^{-1/2}$ **Standard limit**

Particle loss at a rate κ

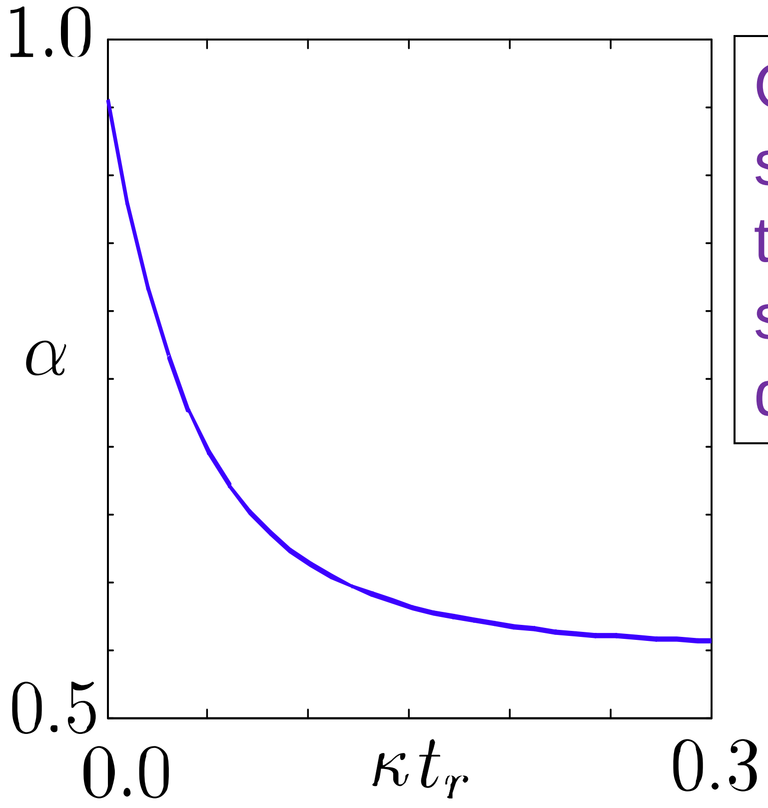

One can obtain Heisenberg limited sensitivity using as input states the twin–Fock states resulting from a slow melting of MI states with two different atoms per lattice site.

M. Rodriguez, S R Clark, D. Jaksch, PRA (R) 75 011601 (2007).

κ $\ll J^2/30V_0$ → Heisenberg-limited sensitivity

III.II

Disordered bosons in a fast oscillatory potential

I. Disordered Bose-Hubbard Model

$$H_0 = -J \sum_j \left(a_j^\dagger a_{j+1} + a_{j+1}^\dagger a_j \right) + \frac{U}{2} \sum_j n_j (n_j - 1)$$

$$+ \frac{W}{2} \sum_j \epsilon_j n_j + C \sum_j j^2 n_j$$

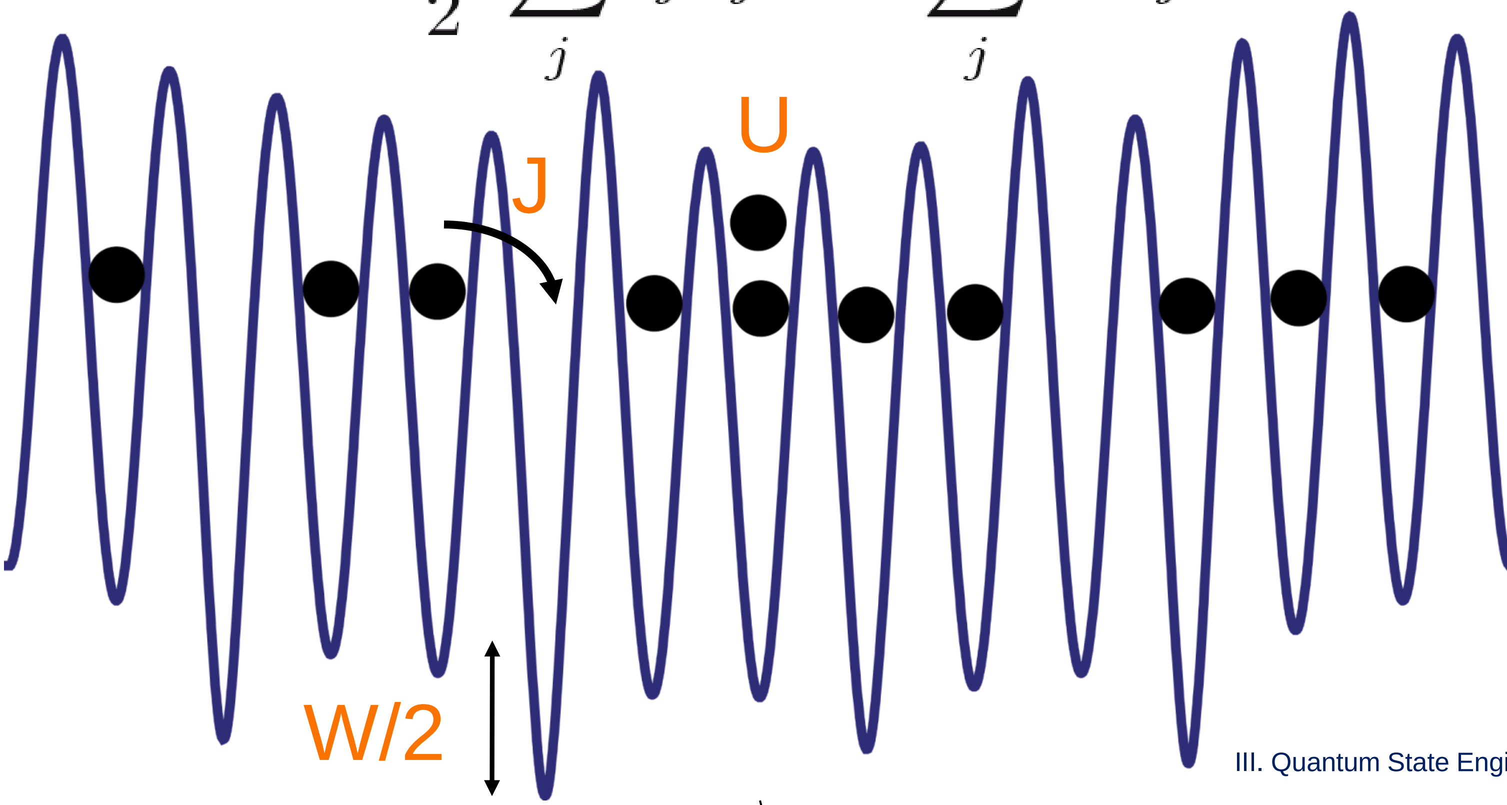

I. Disordered-Bose-Hubbard Model

R. Roth and K. Burnett, Phys. Rev. A 68, 023604 (2003)

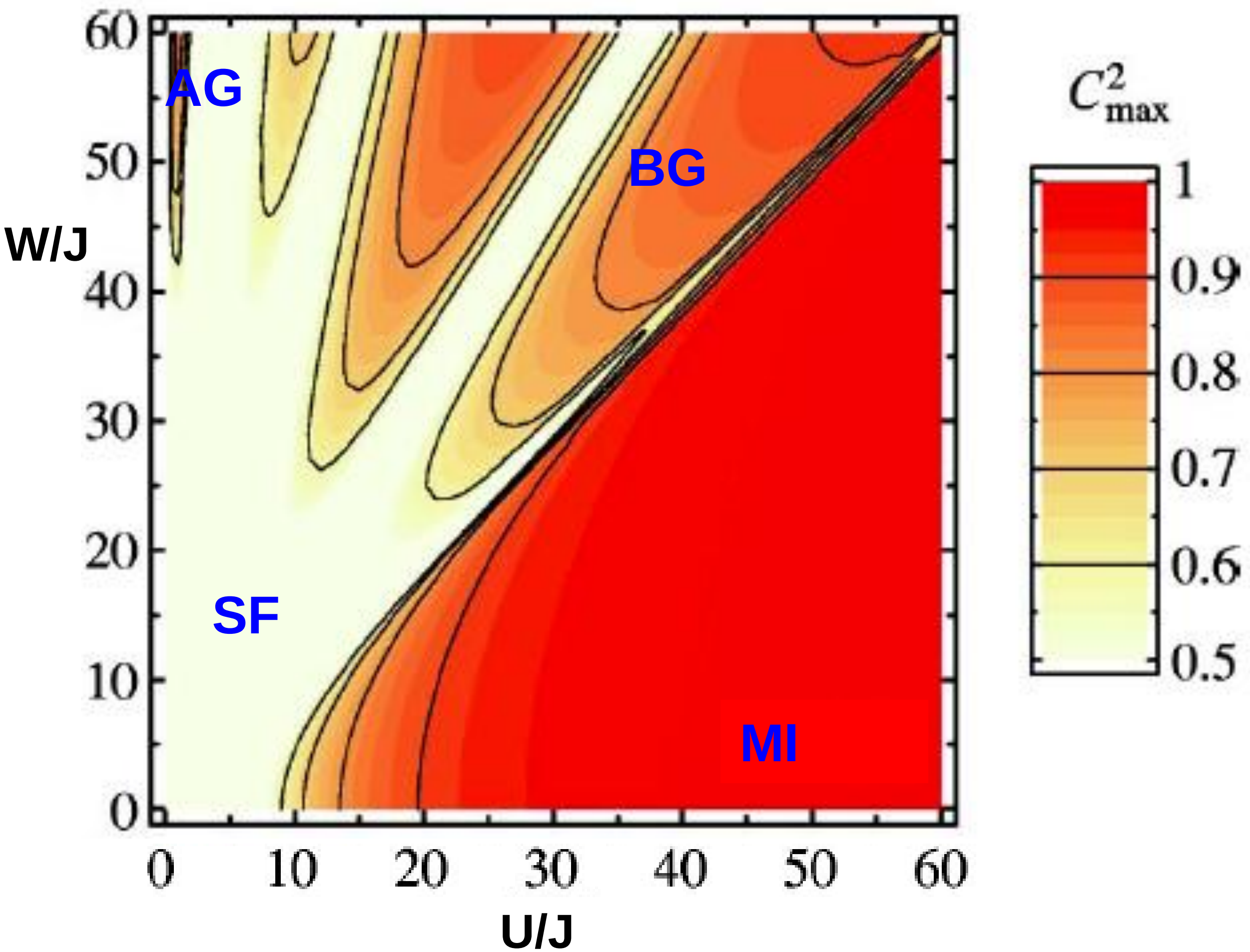

W/U=0

U/J→ ∞ Mott Insulator

U/J→ 0 Superfluid

W/U>0

U/J→ ∞ Insulator

W/U>1 Bose Glass

W/U<1 MI,BG

U/J→ 0 Superfluid

W/U→∞

Anderson Glass

II. Driven DBH model

$$H(t) = H_0 + V(t)$$

$$\boxed{V(t) = V\cos(\omega t + \delta)\sum_j j n_j}$$

- Time-dependent periodic Hamiltonian T=2π/ω

$$i\frac{\partial}{\partial t}|\Psi(t)\rangle = H(t)|\Psi(t)\rangle$$

- Floquet theory

$$H^F \equiv H(t) - i\frac{\partial}{\partial t} \qquad H^F(t)|\phi^e(t)\rangle = e|\phi^e(t)\rangle$$

$$|\phi^e(t)\rangle = |\phi^e(t+T)\rangle$$

II. Floquet theory

- We solve the Schrödinger eq. using the cyclic eigenstates of H_F

$$|\,\Psi(t)\rangle = U(t,t_0;V)\,|\,\Psi(t_0)\rangle \qquad |\,\Psi^e(t)\rangle = e^{-iet}\,|\,\phi^e(t)\rangle$$

$$U(t,t_0;V) = \sum_\alpha |\,\Psi^{\varepsilon_\alpha}(t)\rangle\,\langle\Psi^{\varepsilon_\alpha}(t_0)\,| \quad \varepsilon_\alpha \equiv e_\alpha \in (-\tfrac{1}{2}\omega,\,\tfrac{1}{2}\omega]$$

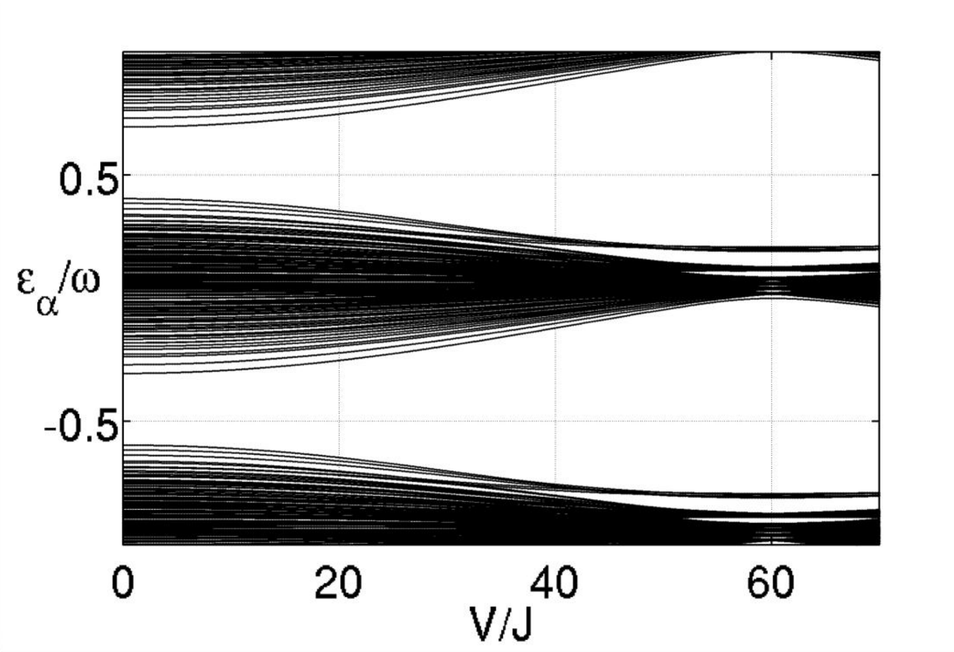

III. Fast oscillatory regime: dynamical suppression of tunneling

$$H_{\text{eff}} = -J_{\text{eff}} \sum_j \left(a_j^\dagger a_{j+1} + a_{j+1}^\dagger a_j \right) + \frac{U}{2} \sum_j n_j (n_j - 1)$$

$$\boxed{J_{eff} = J e^{\pm i V/\omega \sin \delta} \mathcal{J}_0(V/\omega)}$$

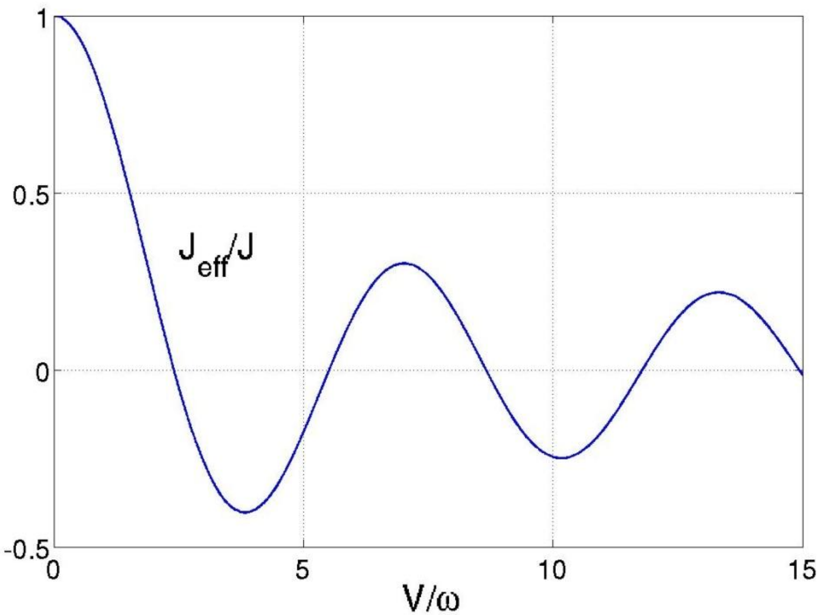

Single particle: Dunlap and Krenke, PRB 34, 3625 (1986).

Many-body :
A. Eckardt, C. Weiss and M. Holthaus PRL 95, 260404 (2005)

Driven Mott-Insulator transition:
one can tune the value of J_{eff}/U to zero driving a fast oscillatory force from 0 to V/ω~2.4

III. Driven SF-MI transition: experimental realization

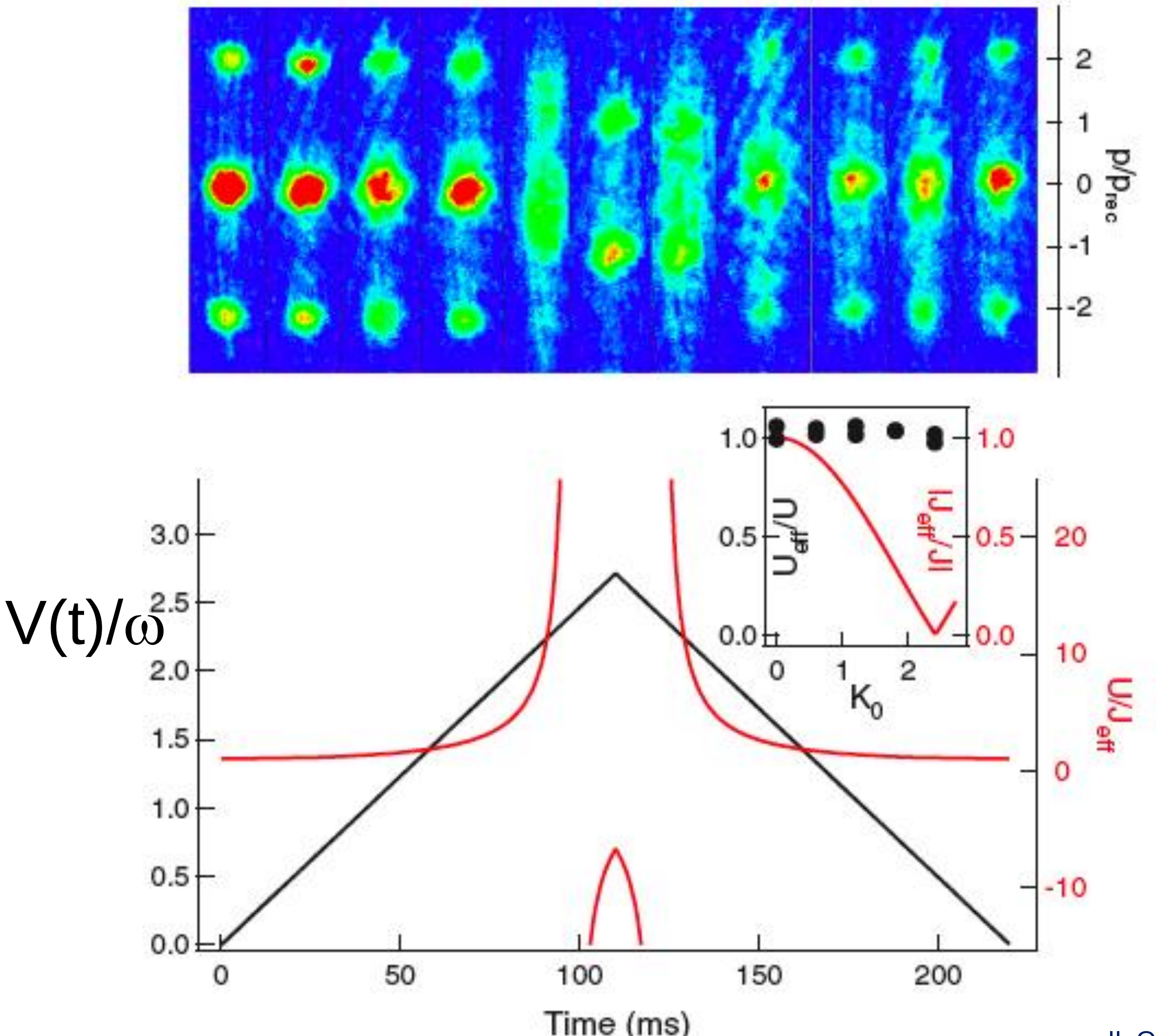

Arimondo's group
PRL 102, 100403 (2009)

III. Fast oscillatory force

Ramping U/J_{eff} and W/J_{eff}

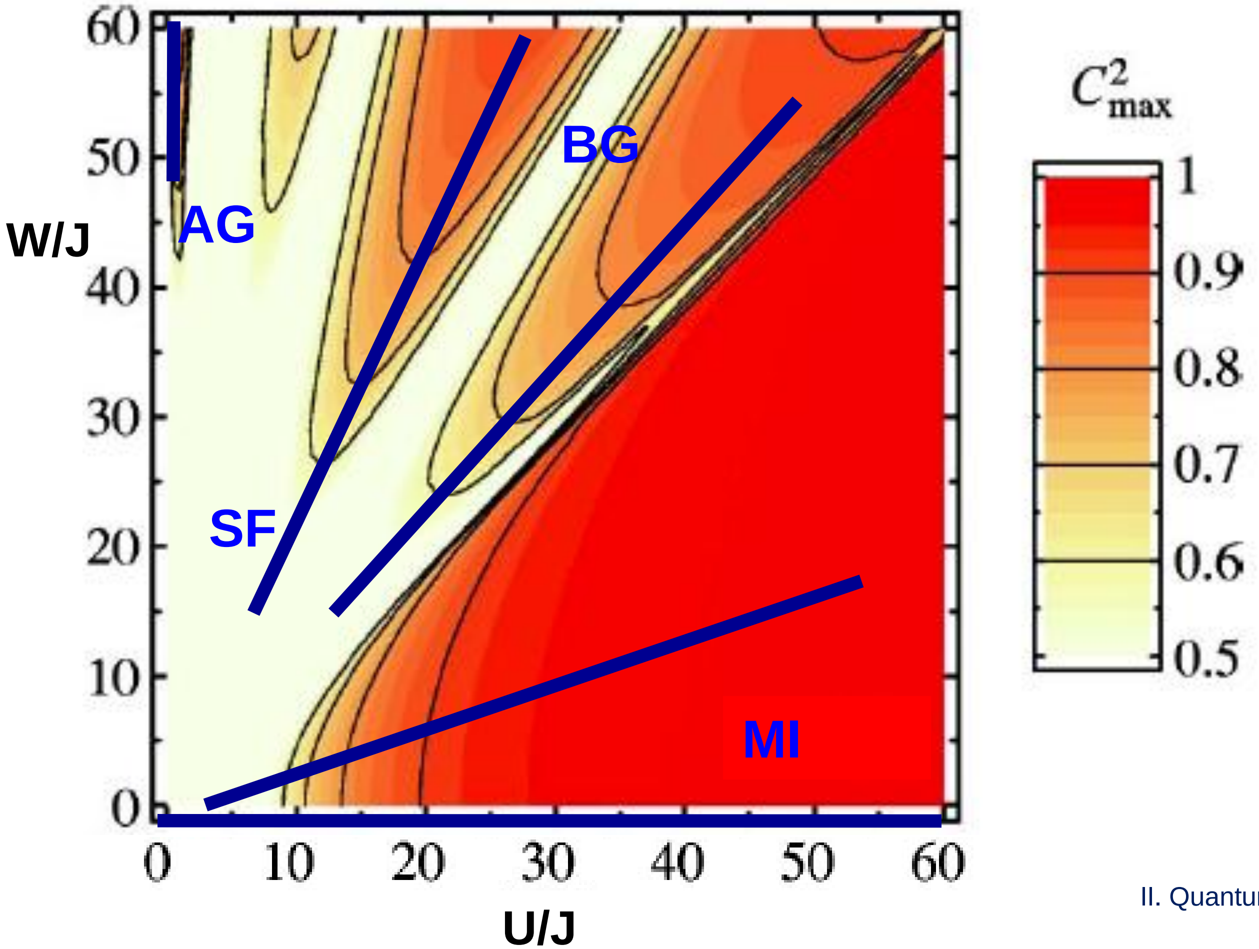

IV. Effect of disorder in quasienergy levels

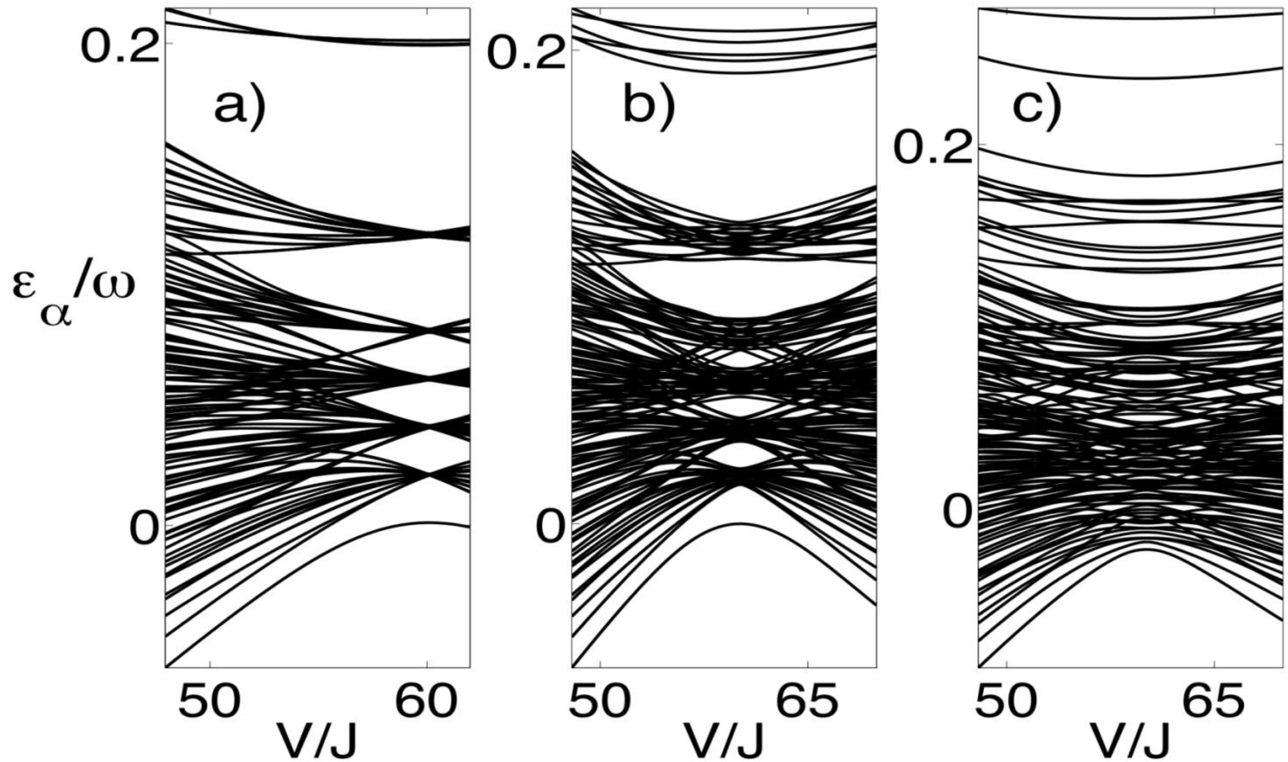

Quasienergy levels of the Floquet Hamiltonian as a function of the strength of the fast oscillatory force V for N=L=5, U/J=0.5 and ω/J=25
a) W/J=0 b) W/J=0.1 and c) W/J=1

IV. Weak disorder: SF-MI transition

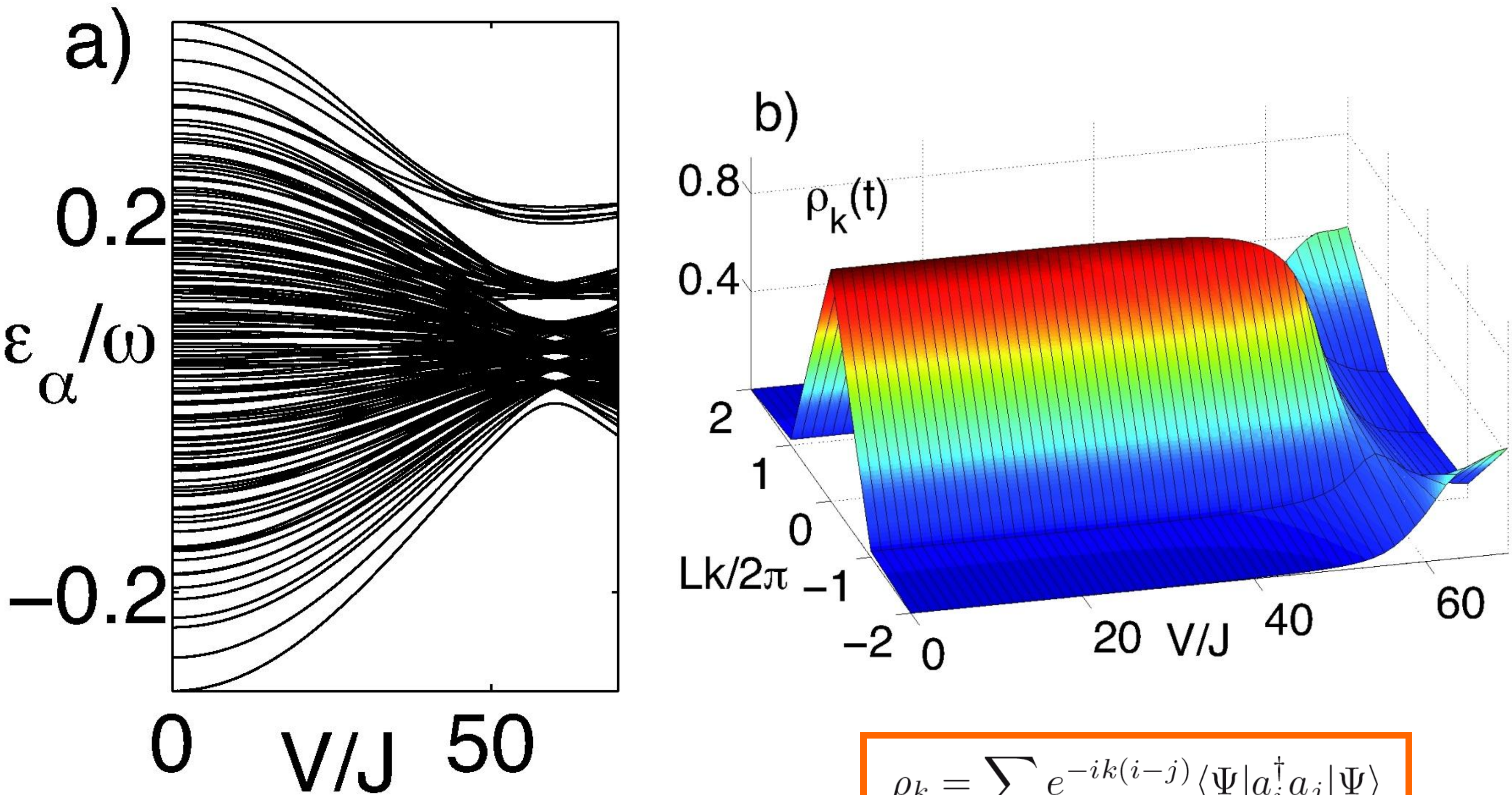

$$\rho_k = \sum_{i,j} e^{-ik(i-j)} \langle \Psi | a_i^\dagger a_j | \Psi \rangle$$

$t_{ramp}J$~200
N=L=5 ω/J=25 W/J=0.1 U/J=0.5

IV. Weak disorder: SF-MI transition

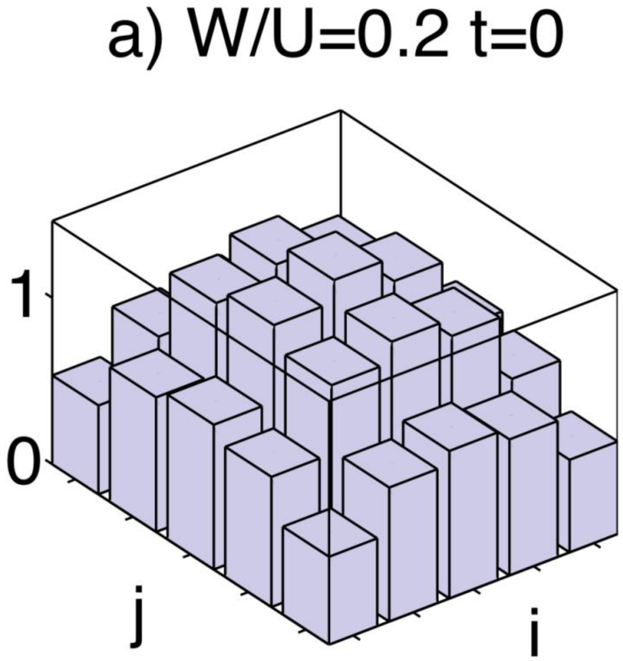

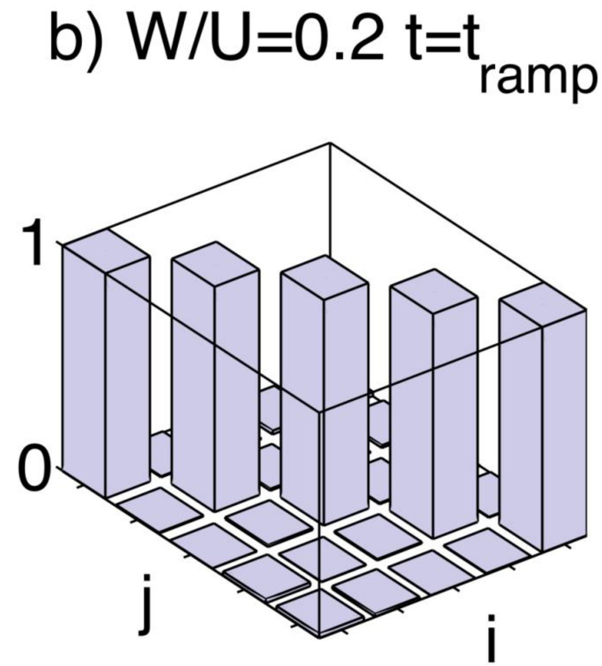

SF

$$\boxed{\rho_{ij} = \langle \Psi | a_i^\dagger a_j | \Psi \rangle}$$

MI

IV. Weak disorder helps to localise for nonconmensurate fillings

SF

MI

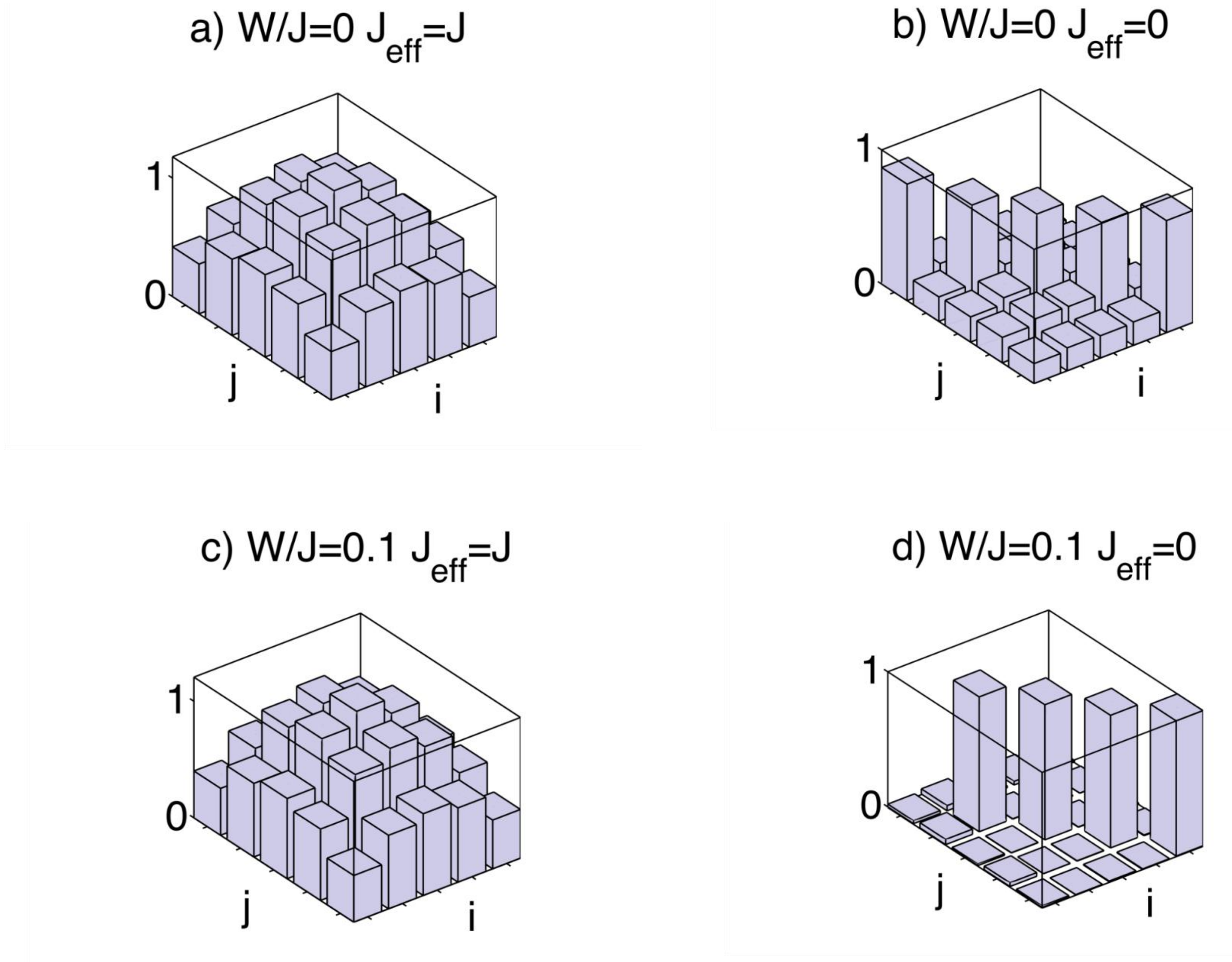

SF

BG

IV. Intermediate disorder: SF-BG

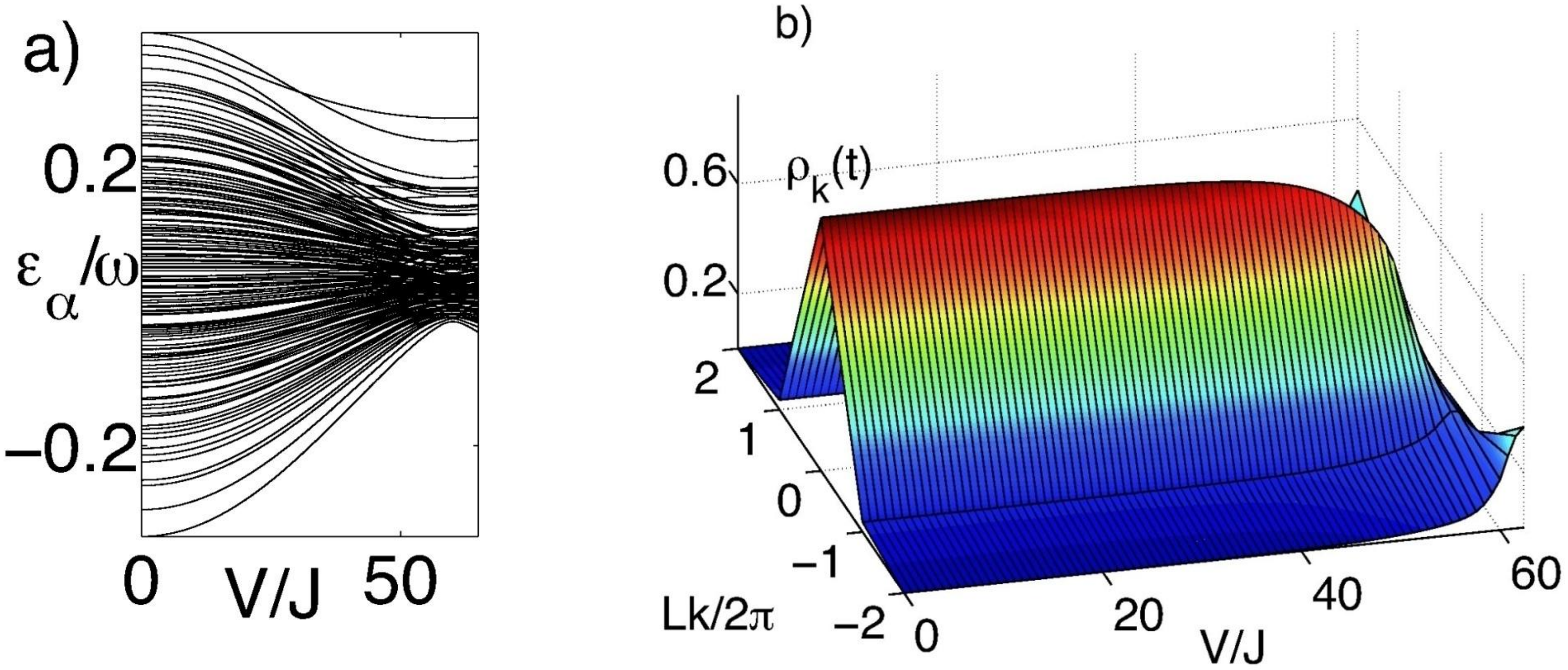

$t_{ramp}J \sim 1500$
N=L=5 ω/J=25 W/J=1 U/J=0.5

IV. Intermediate disorder: SF-BG transition

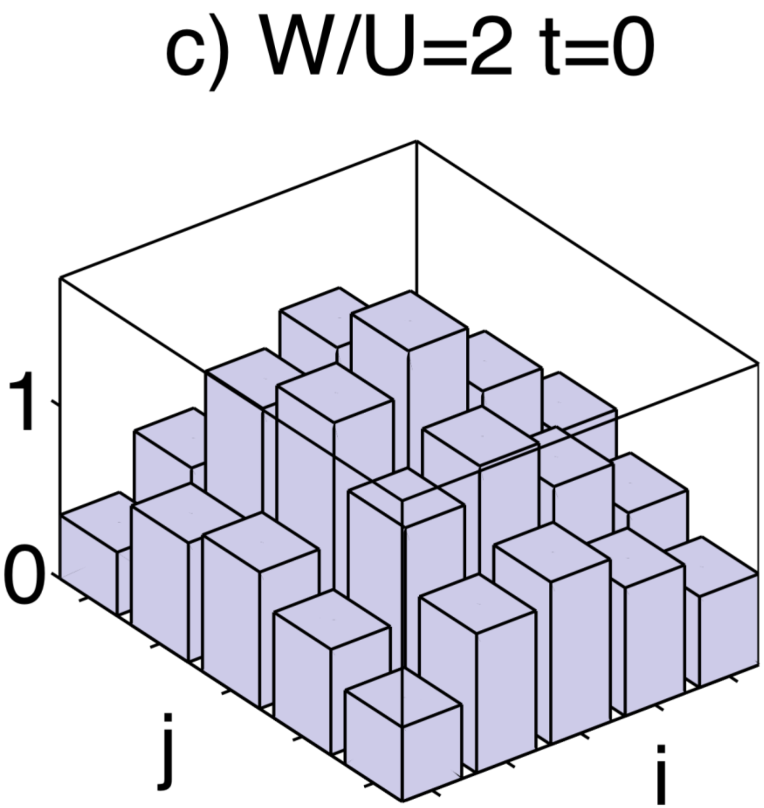

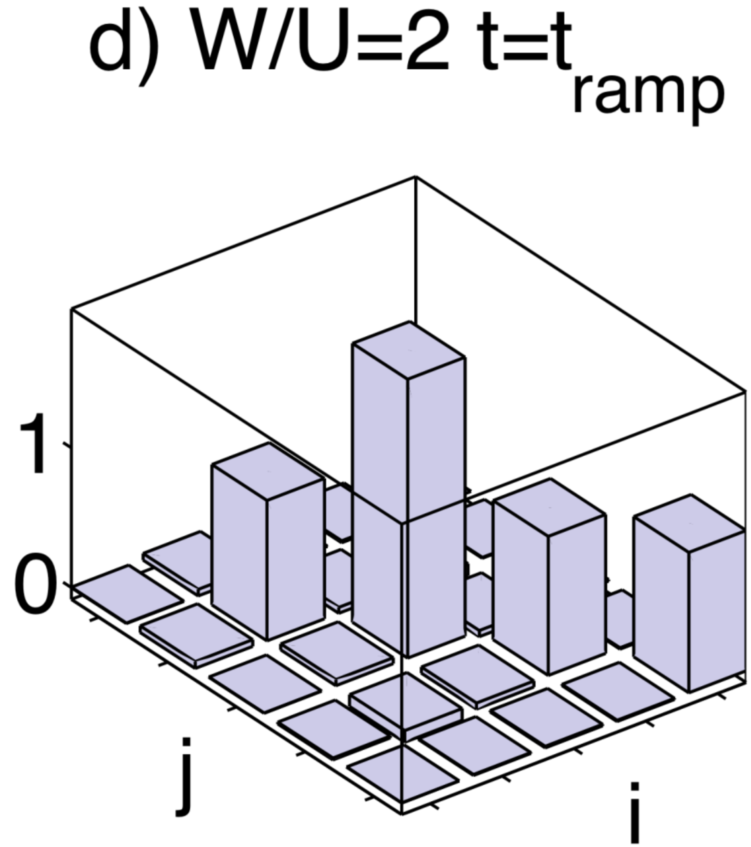

SF

BG

IV Spectra of the final states after ramping

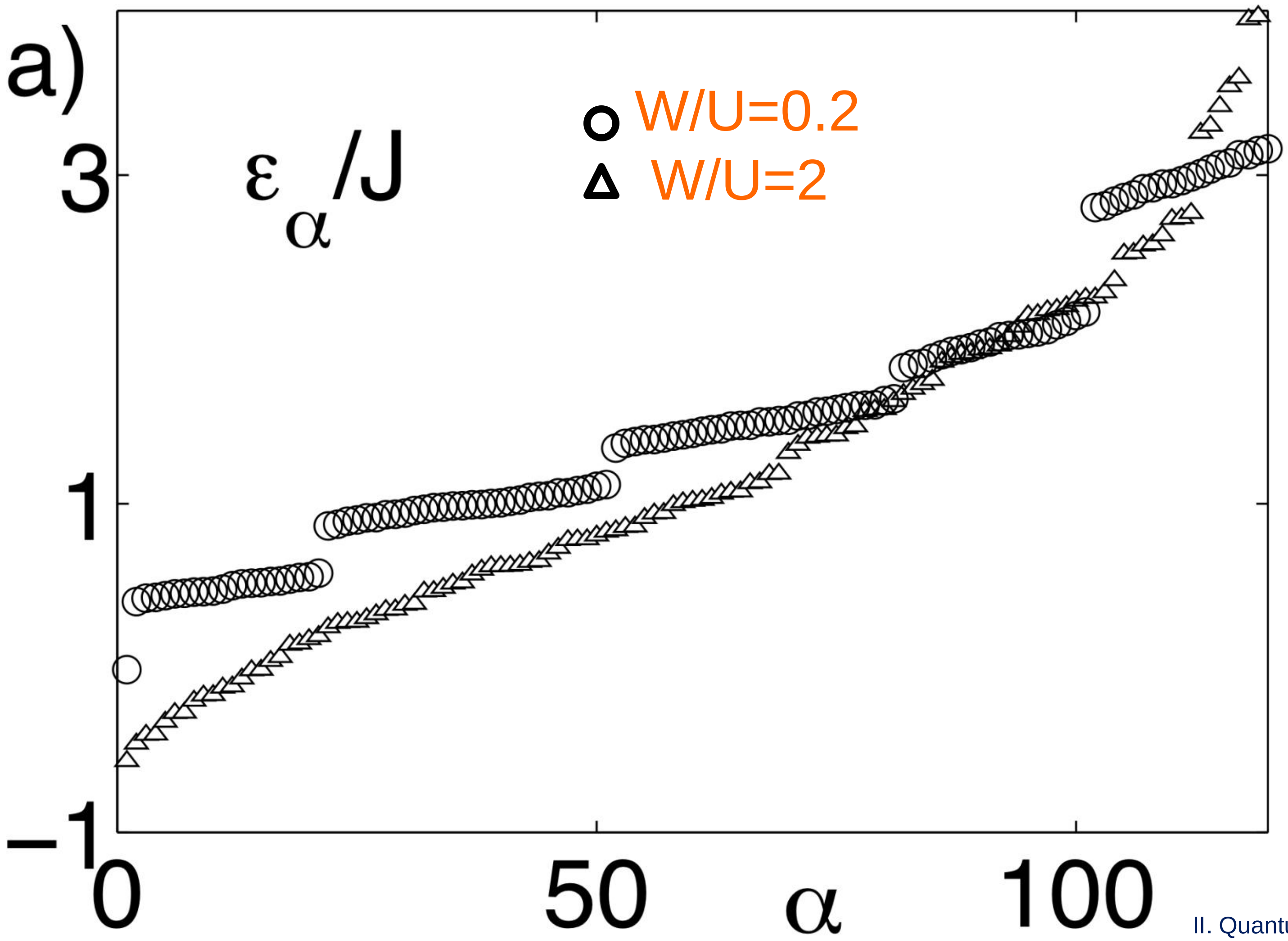

IV Strong disorder: AG-BG

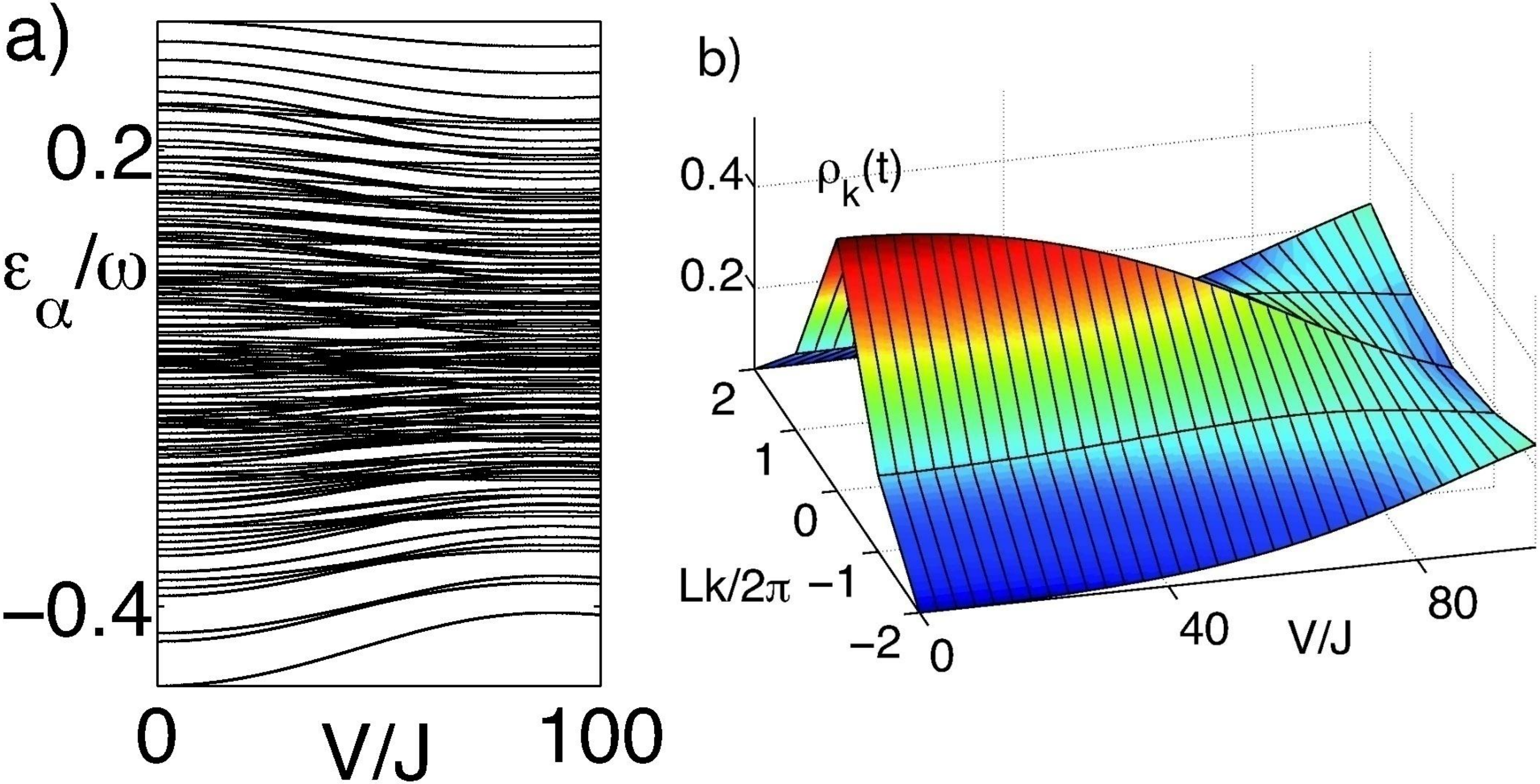

$t_{ramp}J$~50

N=L=5 ω/J=25 W/J=7 U/J=0.05

IV Strong disorder

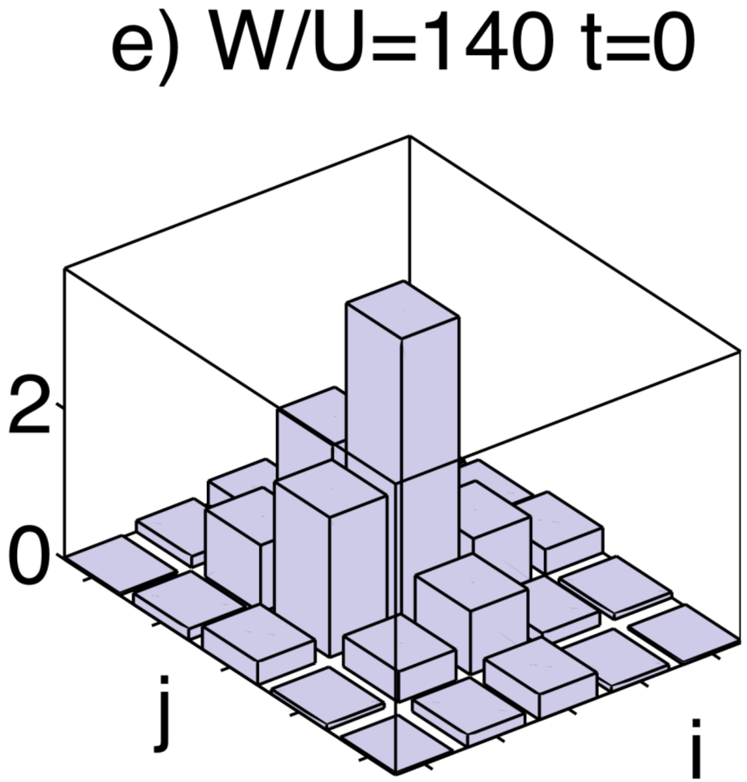

AG

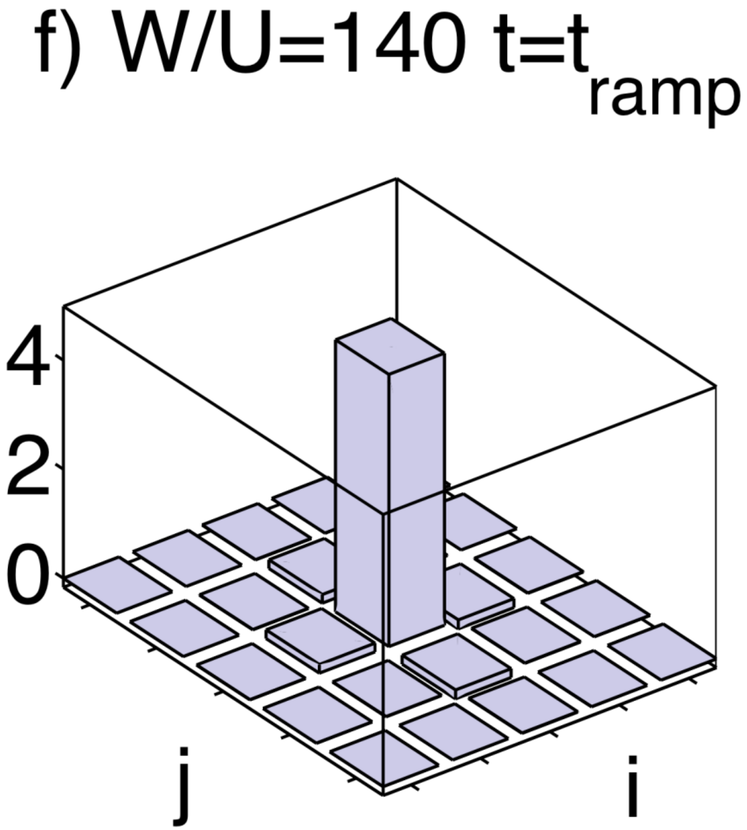

BG

IV Initial state for strong disorder: Anderson Glass

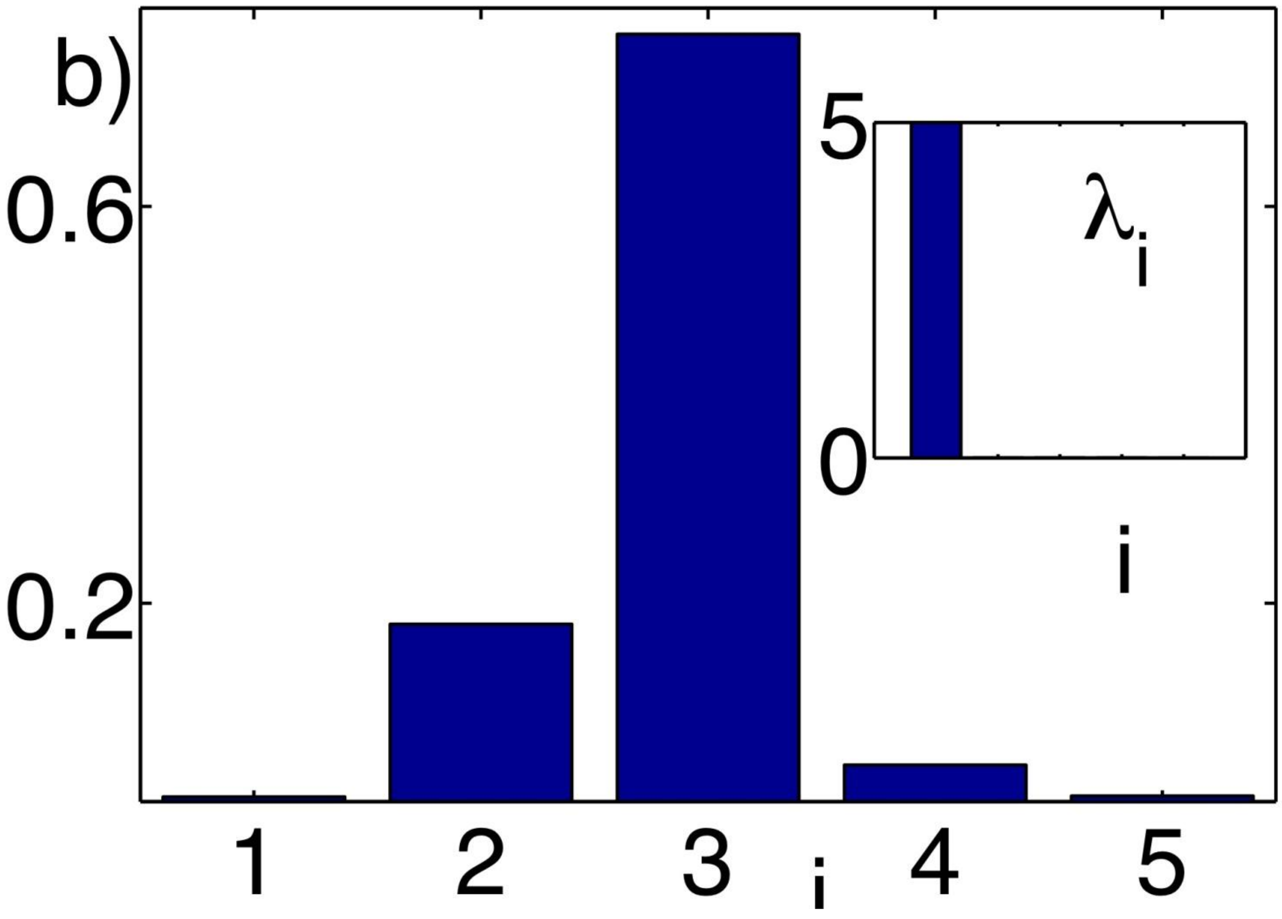

III.II Disordered bosons in a fast oscillatory potential

- A fast oscillatory force results in an effective tunneling
- One can drive adiabatic **dynamical** transitions across the phase diagram in experimentally relevant times

J.Santos, R. Molina, J.Ortigoso, M. Rodríguez, PRA 80,063602 (2009)

III.III
Orientation and alignment of molecules

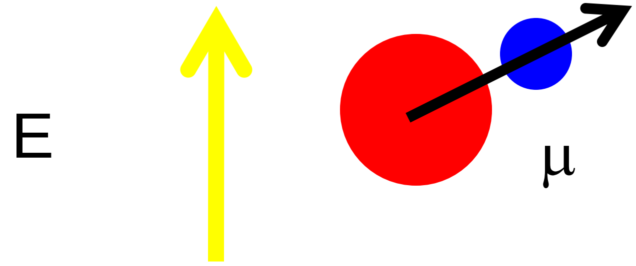

Alignment of molecules with a train of ultrafast laser pulses

Floquet Hamiltonian

$$K(t') = -\imath \frac{\hbar}{B}\frac{\partial}{\partial t'} + \mathbf{J}^2 - (\Delta\omega \cos^2\theta + \omega_\perp) g(t')$$

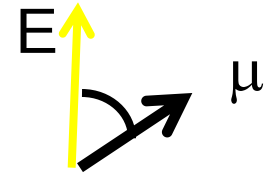

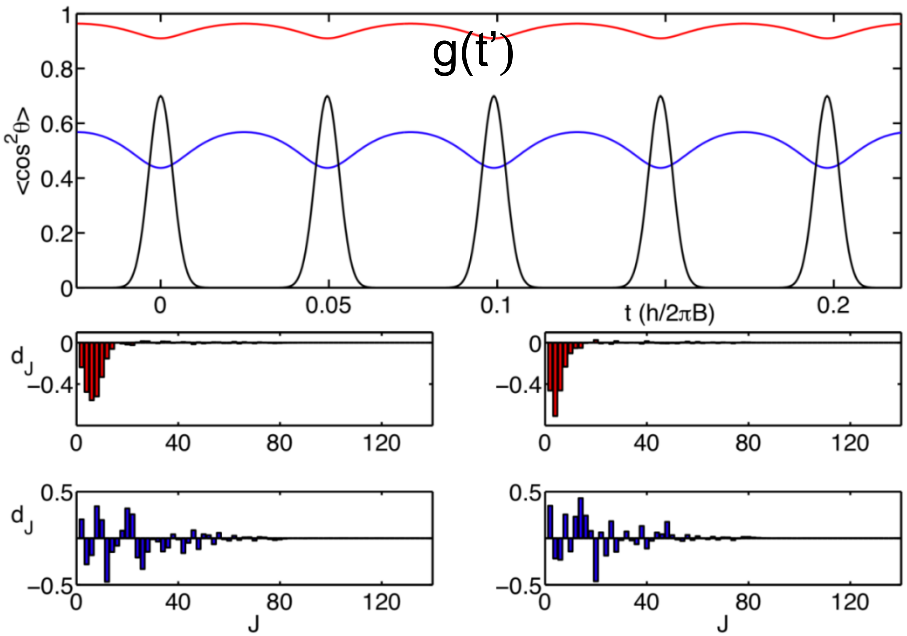

$$|\widetilde{\Psi}(t)\rangle = \exp\left[-\imath\widetilde{\varepsilon}(t-t_0)\right] \sum_{J=0}^{J_{\max}} d_J(t)|J\rangle$$

- Choosing the shape of the pulse train, one obtains rotational wave-packets with different orientation.
- Orientation defines the effective dipole moment of the molecule and thus the long-range dipole-dipole interactions between them.
- → different Hubbard Hamiltonians

J.Ortigoso, M. Rodriguez, JSantos, A. Karpati, V. Szalay Journal of Chemical Physics (2010)

IV.
Detection of strongly correlated states

I. Quantum Spin Polarization Spectroscopy
II. Atom counting

IV.I

Quantum spin polarization spectroscopy

Atom-light interfaces

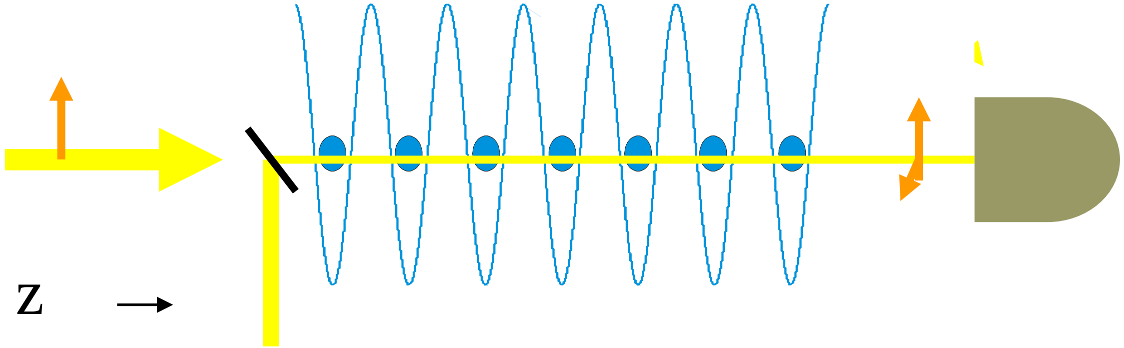

$$\hat{s}_z = \frac{1}{2}\left(\hat{a}_+^\dagger \hat{a}_+ - \hat{a}_-^\dagger \hat{a}_-\right)$$

$$\hat{s}_x = \frac{1}{2}\left(\hat{a}_+^\dagger \hat{a}_- - \hat{a}_-^\dagger \hat{a}_+\right)$$

$$\hat{s}_y = \frac{1}{2i}\left(\hat{a}_+^\dagger \hat{a}_- - \hat{a}_-^\dagger \hat{a}_+\right)$$

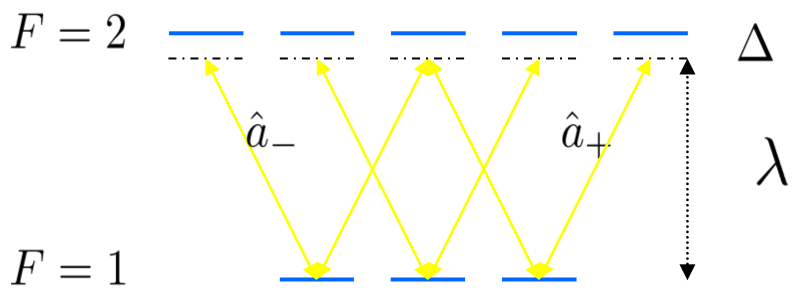

$$\hat{H}_{eff} = -\int d\mathbf{r} a_0 \hat{\mathbf{1}} \hat{\mathbf{1}} + a_1 \hat{s} \hat{J} + a_2[\hat{\mathbf{1}} \hat{J}^2 - \hat{s}_- \hat{J}_+^2 - \hat{s}_+ \hat{J}_-^2]$$

$$\hat{H}_{eff} \sim -\kappa \int d\mathbf{r} \hat{s}_z \hat{J}_z(\mathbf{r})$$

$$a_i \sim n \gamma \lambda^2 c/(16\pi A\Delta)$$

Propagation of light macroscopically polarized in the x-direction: Polarization rotation

$$\boxed{\hat{H}_{eff} \sim -\kappa \int d\mathbf{r}\,\hat{s}_z \hat{J}_z(\mathbf{r})}$$

$$\langle \hat{S}_x^{\text{in}} \rangle = \frac{N_P}{2} \quad \langle \hat{S}_y^{\text{in}} \rangle = \langle \hat{S}_z^{\text{in}} \rangle = 0$$

atoms

$$[\hat{H}_{eff}, \hat{J}_z] = 0$$

→ $< \mathbf{J_z} >$ constant

The collective spin is rotated around the z-axis by $\chi = -\kappa t/\hbar$

light

$$-i\hbar c \partial_{\mathbf{r}} \hat{S}_i = [\hat{S}_i, \hat{H}_{eff}]$$

$$\hat{S}_y^{\text{out}} = \cos\theta \hat{S}_y^{\text{in}} + \sin\theta \hat{S}_x^{\text{in}}$$

$$\hat{S}_x^{\text{out}} = -\sin\theta \hat{S}_y^{\text{in}} + \cos\theta \hat{S}_x^{\text{in}}$$

Faraday rotation of the Stokes operators in the x-y plane

$$\langle \hat{X}_S^{\text{out}} \rangle \sim \langle \hat{J}_z \rangle$$

$$\langle (\Delta \hat{X}_S^{\text{out}})^2 \rangle = \frac{1}{2} + \frac{\kappa^2}{F N_{\text{at}}} \langle (\hat{J}_z - \langle \hat{J}_z \rangle)^2 \rangle$$

Experiments at NIST with F=1 spinor condensates:
Y. Liu et al, PRL 102,125301(2009)

Probing strongly correlated states

Heisenberg Hamiltonian
Spin F=1

$$H=\sum_{\langle n,n'\rangle}\cos\beta\,\hat{\mathbf{j}}(z_n)\cdot\hat{\mathbf{j}}(z_{n'})+\sin\beta\,\left[\hat{\mathbf{j}}(z_n)\cdot\hat{\mathbf{j}}(z_{n'})\right]^2$$

Paramagnetic states

Antiferromagnetic states

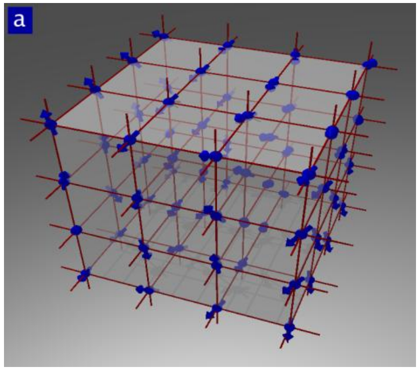

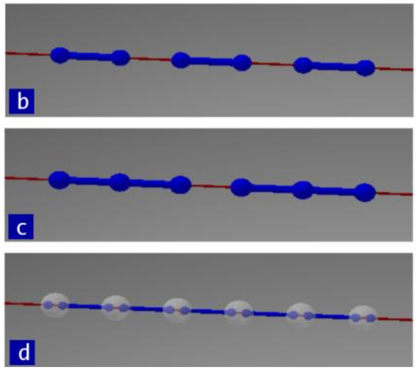

$$\langle\hat{X}_s^{\rm out}\rangle\sim\langle\hat{J}_z\rangle=0$$

$$\langle(\delta\hat{X}_S^{\rm out})^2\rangle-\frac{1}{2}=\frac{\kappa^2}{2N_{\rm at}}\langle(\hat{J}_z-\langle\hat{J}_z\rangle)^2\rangle=\frac{5\kappa^2}{2}$$

$$\langle\hat{X}_S^{\rm out}\rangle\sim\langle\hat{J}_z\rangle=0$$

$$\langle(\delta\hat{X}_S^{\rm out})^2\rangle-\frac{1}{2}=0$$

Spatially resolved probing: access to the effective atomic spin

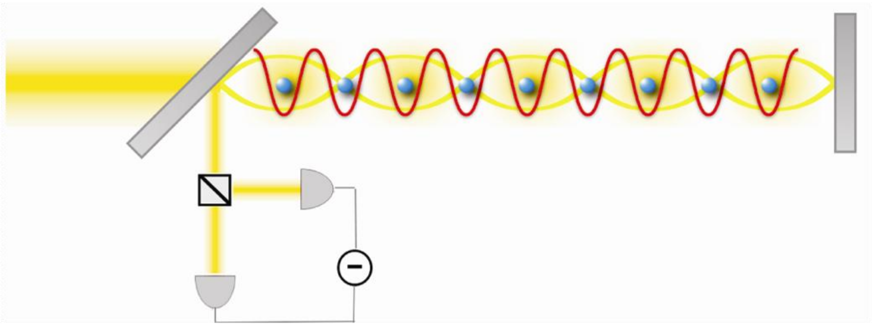

$$\langle \hat{X}_S^{\mathrm{out}} \rangle \sim \langle \hat{J}_z{}^{\mathrm{eff}} \rangle$$

$$\langle (\delta \hat{X}_S^{\mathrm{out}})^2 \rangle = \frac{1}{2} + \frac{\kappa^2}{N_{\mathrm{at}}} \langle (\hat{J}_z{}^{\mathrm{eff}} - \langle \hat{J}_z{}^{\mathrm{eff}} \rangle)^2 \rangle$$

$$\hat{J}_z^{\mathrm{eff}} = \int dz \cos^2(k_P z + \phi) \hat{J}_z(z)$$

Averaging over phases ϕ :

access to the magnetic structure factor

$$\langle (\delta \hat{X}_S^{\mathrm{out}}(\mathbf{k})^2 \rangle = \frac{1}{2} + \frac{\kappa^2 V}{4 N_{\mathrm{at}}} [4 S_m(0) + S_m(2\mathbf{k}) + S_m(-2\mathbf{k})]$$

$$S_m(\mathbf{k}) = \frac{1}{V} \int \mathbf{r} \int \mathbf{r'} e^{-i\mathbf{k}(\mathbf{r}-\mathbf{r'})} \langle \delta \hat{J}_z(\mathbf{r}) \delta \hat{J}_z(\mathbf{r'}) \rangle$$

Standing-wave probing of F=1 antiferromagnetic states

Dimer

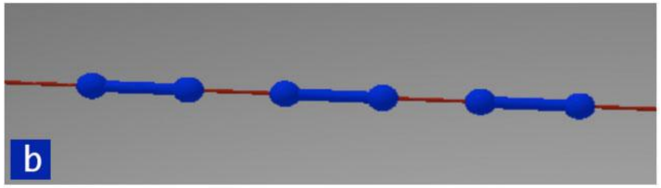

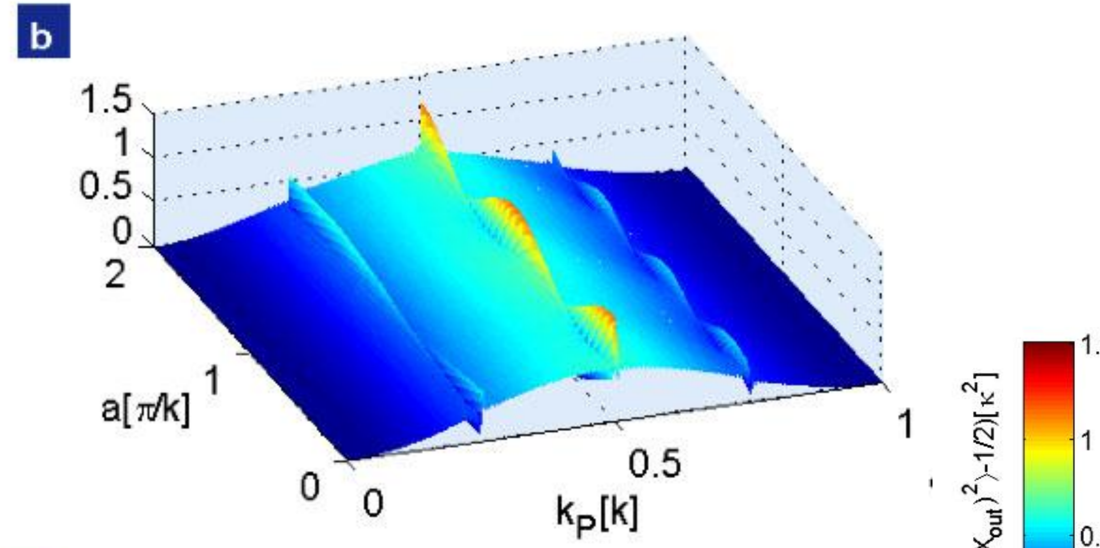

Trimer

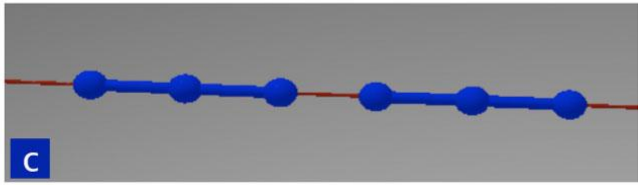

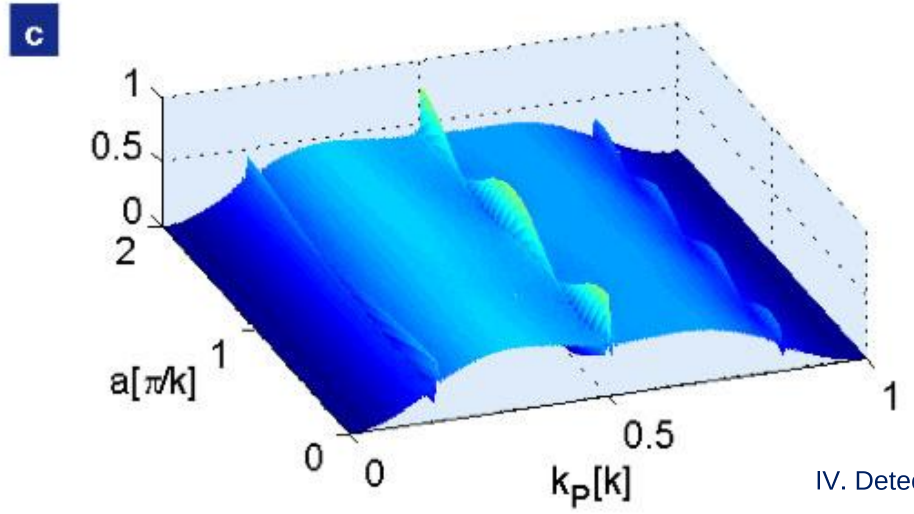

Magnetic structure factor for attractive fermions

$$H = -t \sum_{i,\sigma} \left(\hat{c}^{\dagger}_{i,\sigma} \hat{c}_{i+1,\sigma} + \mathrm{h.c.} \right) - U \sum_{i} \hat{n}_{i\uparrow} \hat{n}_{i\downarrow}$$

FFLO pairs with momentum $Q = k_{F\uparrow} - k_{F\downarrow}$

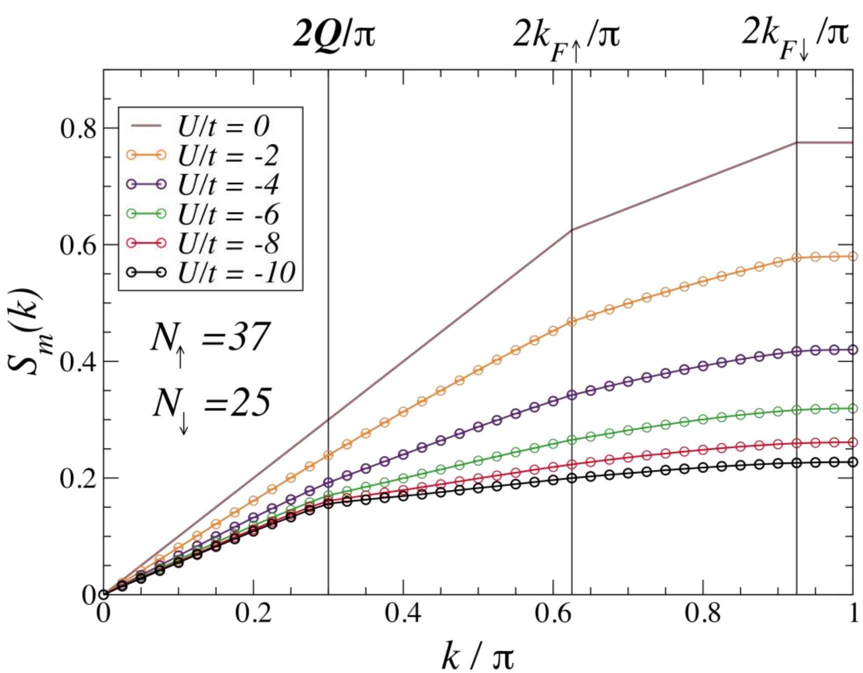

QMC calculation

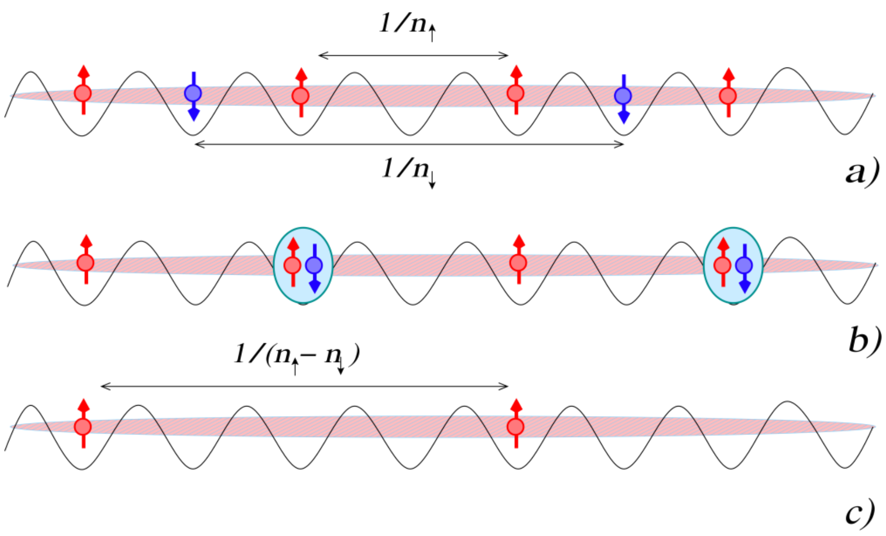

IV.I Quantum Polarization Spectroscopy

- QPS can be used to distinguish strongly correlated antiferromagnetic phases of the spin-1 Heisenberg Hamiltonian

- Can distinguish superfluidity and the FFLO phase in a 1D chain of attractive fermions

Eckert et al, PRL 98, 100404 (2007)

K. Eckert, O. Romero-Isart, M. Rodríguez,M Lewenstein, E S Polzik, A. Sanpera, Nature Physics 4, 50 (2008)

T. Roscilde, M. Rodríguez, K. Eckert, O. Romero-Isart, M. Lewenstein, E S Polzik, A. Sanpera New Journal Physics (2009)

IV.II-Counting statistics of atoms

- After expansion

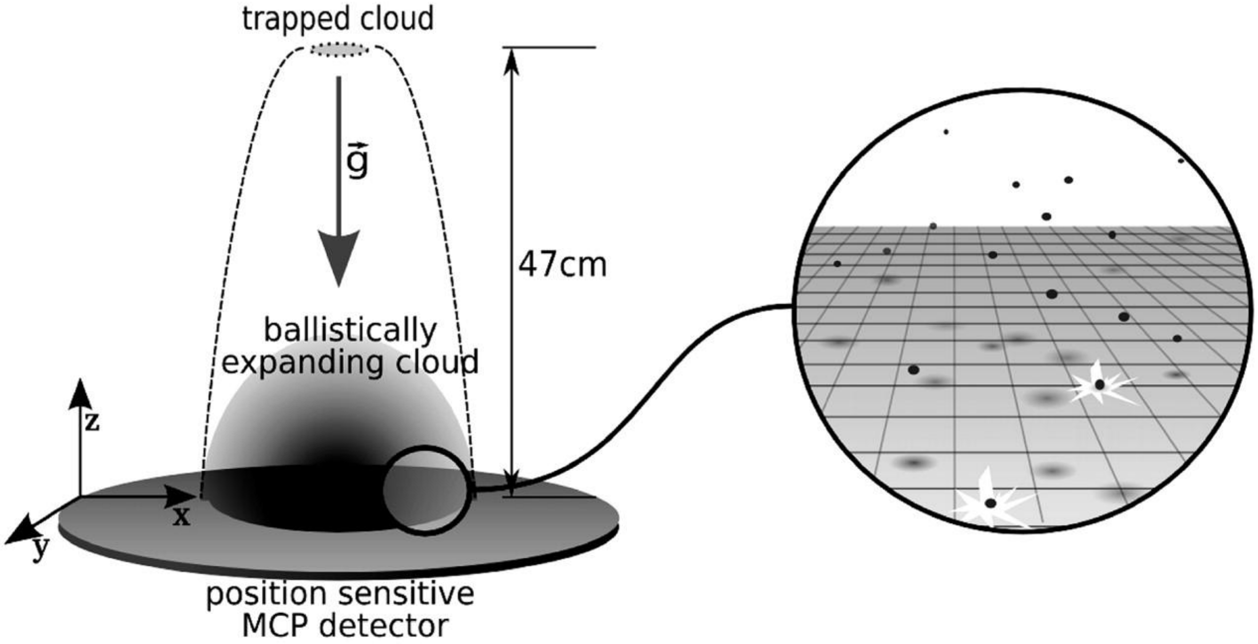

- In the lattice

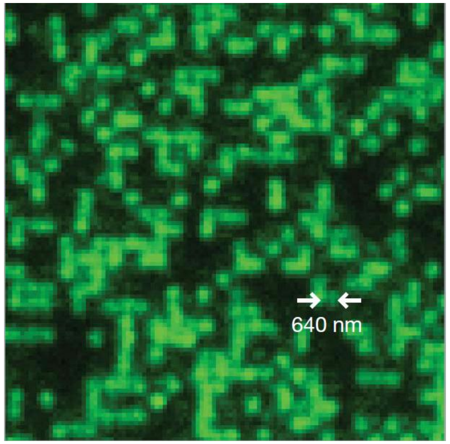

M.Schellekens et al Science 310, 648 (2005)

Greiner's group Nature 462 2009
Bloch's group Nature 467 2010
Chen's group Nature 460 2009

Counting formalism [Kelley & Kleiner 1964, Glauber 1965]

The probability distribution of counting m fermionic/ bosonic atoms

$$p(m) = \frac{(-1)^m}{m!} \frac{d^m}{d\lambda^m} \mathcal{Q} \Big|_{\lambda=1}$$

can be derived from a generating function

$$\mathcal{Q}(\lambda) = \mathrm{Tr}(\rho : e^{-\lambda \mathcal{I}} :).$$

with the normal/appex order of the intensity of the atoms at the detector

$$\mathcal{I} = \int_0^t dt' \int d\mathbf{r}' \Omega(\mathbf{r}') \tilde{\Psi}^\dagger(\mathbf{r}', t') \tilde{\Psi}(\mathbf{r}', t')$$

Fermion and spin counting

$$\hat{H} = -J\sum_{j=1}^{N}(\hat{c}_j^\dagger\hat{c}_{j+1} + \gamma\hat{c}_j^\dagger\hat{c}_{j+1}^\dagger + h.c. - 2g\hat{c}_j^\dagger\hat{c}_j + g).$$

$$H_{xy} = -J\sum_{j=1}^{N}\left[(1+\gamma)S_j^x S_{j+1}^x + (1-\gamma)S_j^y S_{j+1}^y + gS_j^z\right]$$

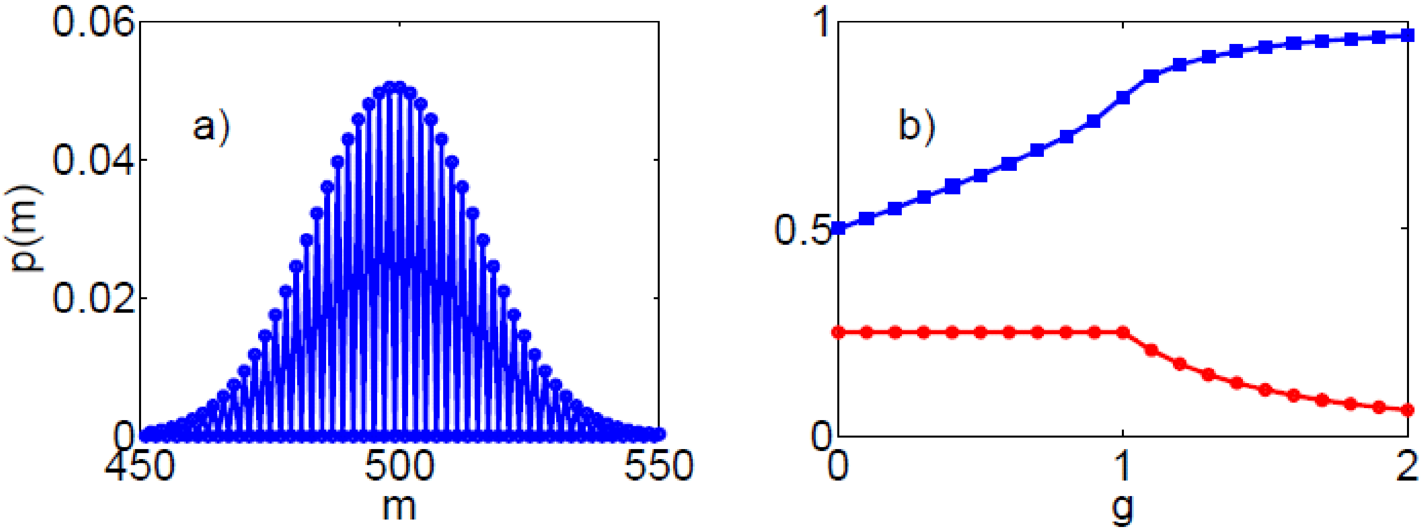

Figure 5.1: a) Counting probability distribution $p(m)$ of finding m particles as a function of m for the fermionic system eq. (5.1) with $\gamma = \kappa$=1, $g = 0$ and $N = 1000$. b) Mean $\bar{m}/N$ (blue squares) and variance σ^2/N (red circles) of the counting distribution as a function of the transverse field g.

S. Braungardt, A. Sen, U. Sen, R. Glauber, M, Lewenstein PRA 78 (2008)

Detection of the QPT

$$H_{xy} = -J \sum_{j=1}^{N} \left[(1+\gamma) S_j^x S_{j+1}^x + (1-\gamma) S_j^y S_{j+1}^y + g S_j^z \right]$$

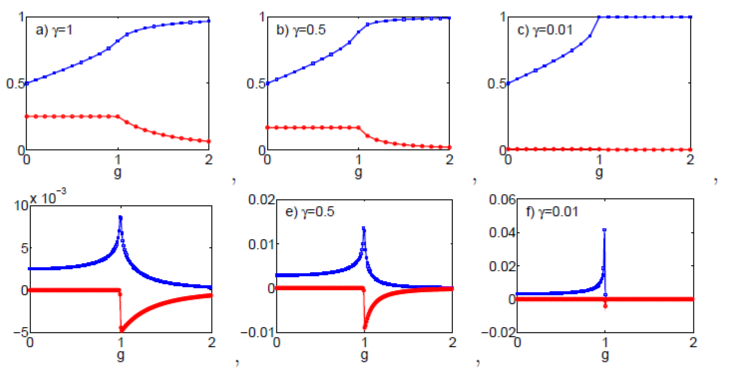

Figure 5.4: (Color online.) a)-c) Mean $\overline{m}/N$ (blue squares) and variance var/N (red circles) of the fermion counting distribution as a function of g for $\kappa = 1$, and indicated values of γ. d)-f) Derivatives of the mean (blue squares) and variance (red circles) for the respective values of γ

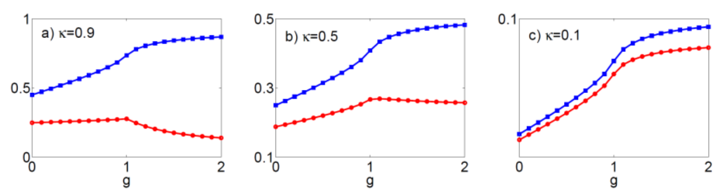

Figure 5.3: (Color online.) Mean $\overline{m}/N$ (blue squares) and variance var/N (red circles) of the fermion counting distribution as a function of g for $\gamma = 1$ (Ising model), and the indicated values of κ.

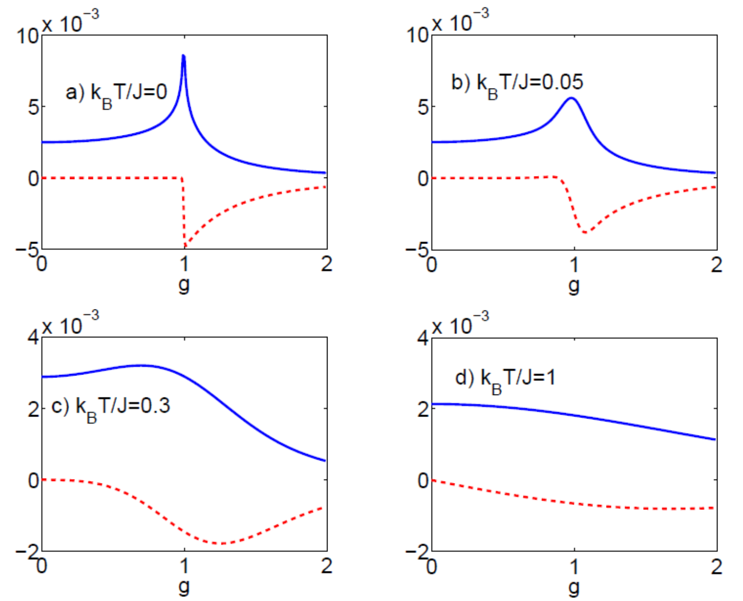

Figure 6.2: Derivative of the mean $\bar{m}/N$ (blue squares) and the variance σ^2/N (red circles) of the counting distribution of the fermionic system eq.(5.1) with $\gamma = 1$ as a function of the transverse field g. a) $k_BT/J = 0$, $N_d = 0$ for all g; b) $k_BT/J = 0.05$ and $N_d/N \simeq 0$ at $g = 0$; c) $k_BT/J = 0.3$ and $N_d/N = 0.03$ at $g = 0$; d) $k_BT/J = 1$ and $N_d/N = 0.27$ at $g = 0$.

S. Braungardt, A. Sen, U. Sen, R. Glauber, M, Lewenstein PRA 78 (2008)
S. Braungardt, M. Rodriguez, A. Sen, U. Sen, R. Glauber, M, Lewenstein PRA 83 (2011)

Counting bosons after expansion

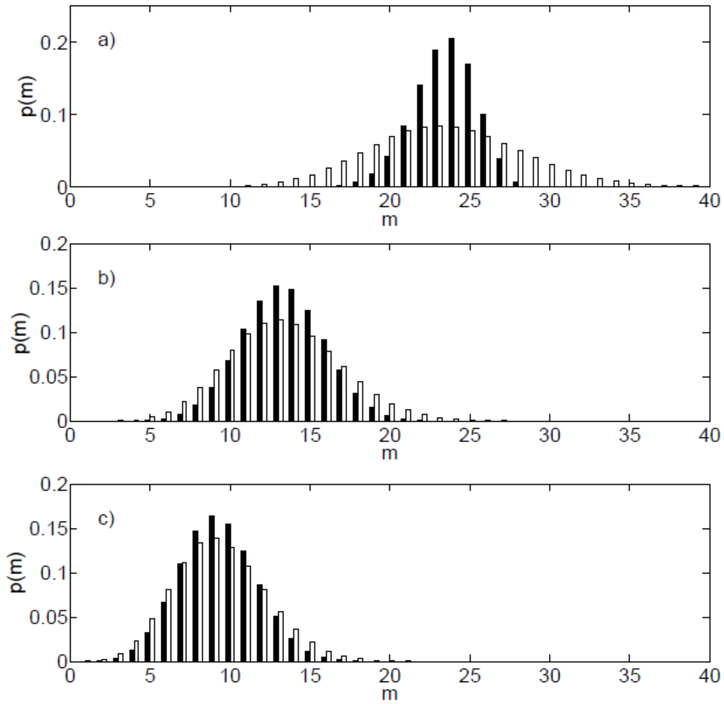

Figure 7.3: MI vs. SF as a function of distance from detector. Probability distribution for MI (black bars) and superfluid (white bars) states in a 3x3x3 lattice. $\Delta_x = \Delta_y = 2$ mm, $\Delta_z = 2$ cm, $\kappa = 1$. a) $Z_0 = 1cm$, b) $Z_0 = 3$ cm, c) $Z_0 = 5$ cm

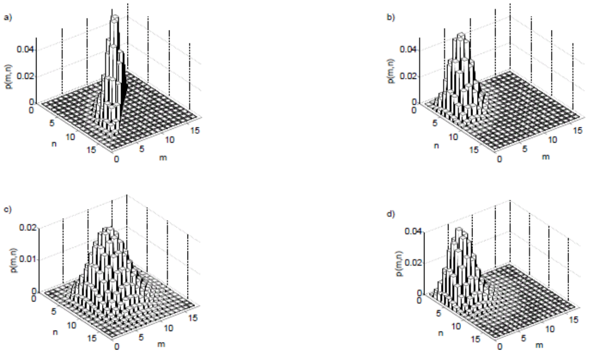

Figure 7.5: Joint probability distribution of an expanded MI (upper row) and a SF (lower row) in a 4x4 lattice with two symmetrically placed detectors. In fig. a) and c), the two detectors overlap at the center of the lattice in x-y direction. In fig. b) and d) the detectors are separated by $d = 1$ cm. $Z_0 = 1cm$, $\Delta_z = 2$ mm, $\Delta_x = \Delta_y = 2$ cm, $\kappa = 0.5$.

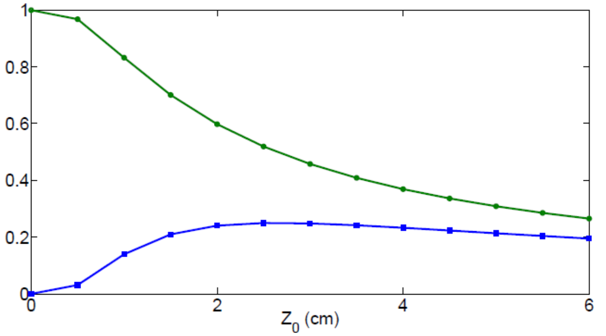

Figure 7.4: var$(m)/N$ of the counting distribution for the MI (blue squares) and SF (green circles) state with respect to the distance from the detector Z_0. $\Delta_x = \Delta_y = 2$ mm, $\Delta_z = 2$ cm, $\kappa = 1$.

S. Braungardt, M. Rodriguez, A. Sen, U. Sen, M, Lewenstein (to be submitted)

V.
QI processing with OL

1. Atoms
2. Molecules

I. Entangling quantum gates O. Mandel et al, Nature 425 (2003)

$$\frac{1+e^{-i\varphi}}{2}|1\rangle_j|1\rangle_{j+1} + \frac{1-e^{-i\varphi}}{2}(|0\rangle_j(|0\rangle_{j+1} - |1\rangle_{j+1}) + |1\rangle_j(|0\rangle_{j+1} + 1\rangle_{j+1}))/2$$

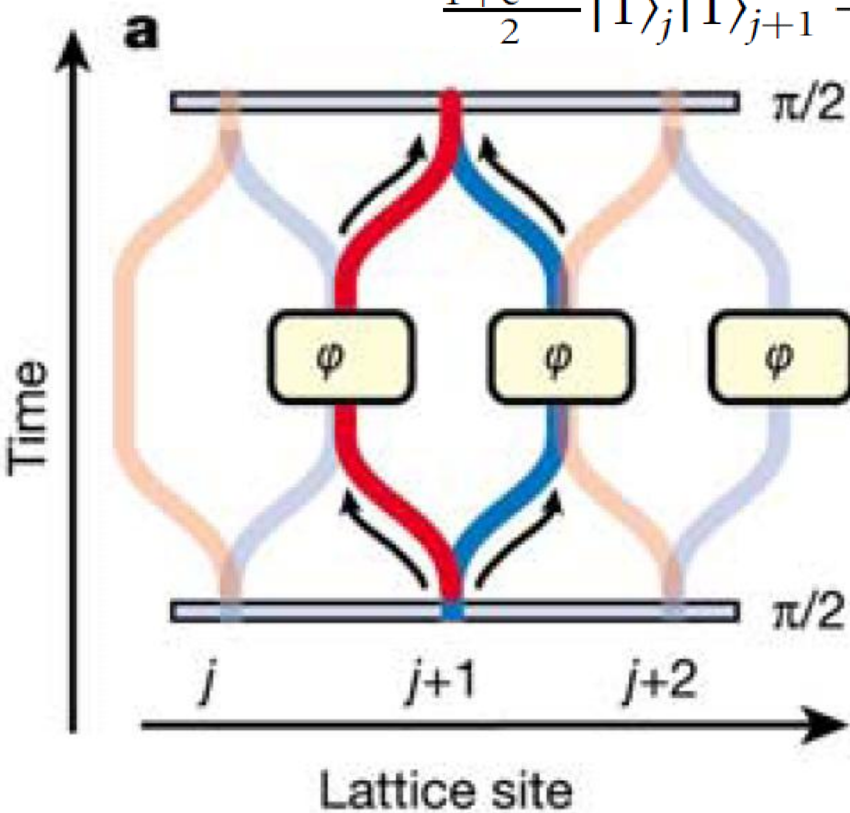

$$(|0\rangle_j|0\rangle_{j+1} + |0\rangle_j|1\rangle_{j+2} + e^{-i\varphi}|1\rangle_{j+1}|0\rangle_{j+1} + |1\rangle_{j+1}|1\rangle_{j+2})/2$$

$$(|0\rangle_j + |1\rangle_j)(|0\rangle_{j+1} + |1\rangle_{j+1})/2$$

$$|0\rangle_j|0\rangle_{j+1}$$

Signature: visibility of the Ramsey fringes

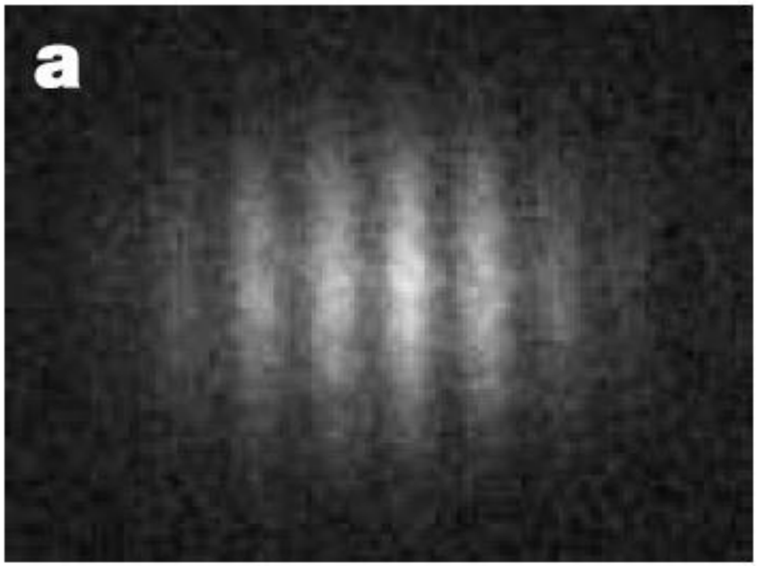

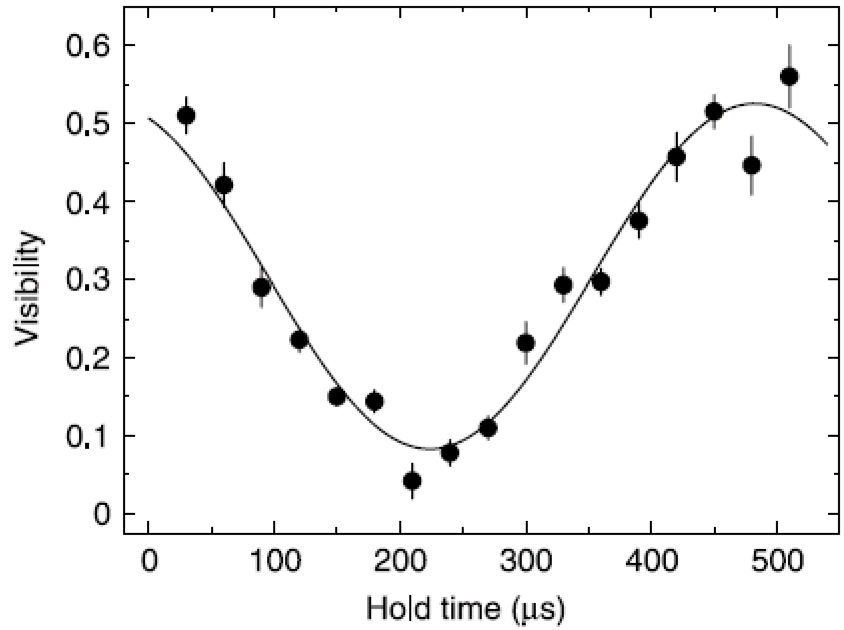

O. Mandel et al, Nature 425 (2003)

I. Swap gate via control of the exchange interaction

M. Anderlini et al, Nature 448 (2007)

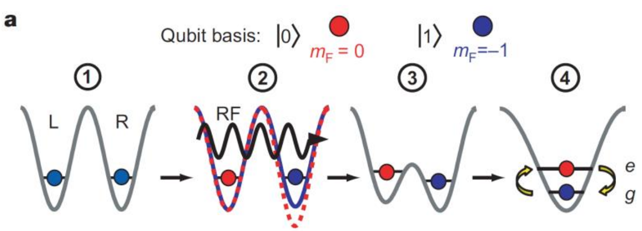

$$|\psi_S\rangle = \phi_S(\mathbf{x}_1,\mathbf{x}_2)|S\rangle = \left(|1_e,0_g\rangle - |0_e,1_g\rangle\right)/\sqrt{2}$$

$$|\psi_T^0\rangle = \phi_T(\mathbf{x}_1,\mathbf{x}_2)|T^0\rangle = \left(|1_e,0_g\rangle + |0_e,1_g\rangle\right)/\sqrt{2}$$

$$|\psi_T^-\rangle = \phi_T(\mathbf{x}_1,\mathbf{x}_2)|T^-\rangle = |0_e,0_g\rangle$$

$$|\psi_T^+\rangle = \phi_T(\mathbf{x}_1,\mathbf{x}_2)|T^+\rangle = |1_e,1_g\rangle$$

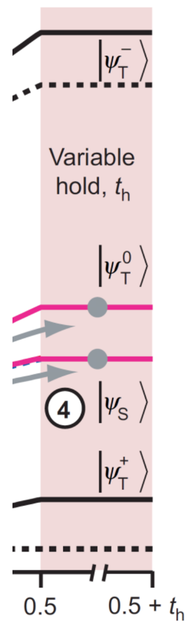

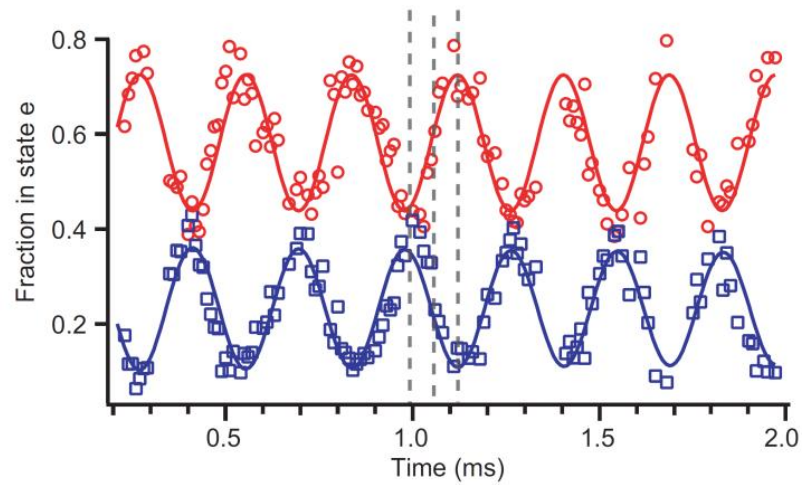

Table 1 | Truth table for SWAP and $\sqrt{SWAP}$ gates

Initial	State after time t	$\sqrt{SWAP}$ $t=\pi\hbar/2U_{eg}=T_{SWAP}/2$	SWAP $t=\pi\hbar/U_{eg}\equiv T_{SWAP}$
$\|0_e,0_g\rangle$	$e^{-iU_{eg}t/2\hbar}\|0_e,0_g\rangle$	$e^{-i\pi/4}\|0_e,0_g\rangle$	$\|0_e,0_g\rangle$
$\|0_e,1_g\rangle$	$\cos(U_{eg}t/2\hbar)\|0_e,1_g\rangle - i\sin(U_{eg}t/2\hbar)\|1_e,0_g\rangle$	$(\|0_e,1_g\rangle - i\|1_e,0_g\rangle)/\sqrt{2}$	$\|1_e,0_g\rangle$
$\|1_e,0_g\rangle$	$-i\sin(U_{eg}t/2\hbar)\|0_e,1_g\rangle + \cos(U_{eg}t/2\hbar)\|1_e,0_g\rangle$	$(-i\|0_e,1_g\rangle + \|1_e,0_g\rangle)/\sqrt{2}$	$\|0_e,1_g\rangle$
$\|1_e,1_g\rangle$	$e^{-iU_{eg}t/2\hbar}\|1_e,1_g\rangle$	$e^{-i\pi/4}\|1_e,1_g\rangle$	$\|1_e,1_g\rangle$

The table ignores a global phase factor $e^{-iU_{eg}t/2\hbar}$.

III. Quantum computation with trapped polar molecules

De Mille, PRL 88 (2002)

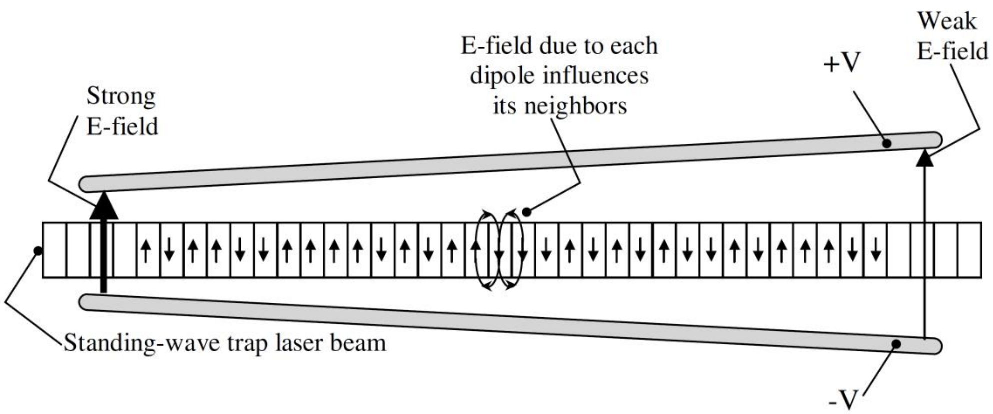

$|\uparrow\rangle_i$

ν_i

$|\downarrow\rangle_i$

i

Single qubit operation

$\nu_i = \nu_0 + d_{eff} E_i / h$

$\nu_0 = hBJ(J+1)$

$d_{eff} = d_g - d_e$

$E_i = E_0 + V\, i$

ν_i in the GHz regime

CNOT gate

Dipole dipole interactions $E_{int} = -\Sigma_j\, d_{eff}/|x_i - x_j|^3$

$|\downarrow\rangle_i |\uparrow\rangle_{i+1}$ $\quad$ $|\uparrow\rangle_i |\uparrow\rangle_{i+1}$

$\nu_{i+1} - d_{eff}^2/(\lambda/2)^3$ $\quad$ $\nu_{i+1} + d_{eff}^2/(\lambda/2)^3$

$|\downarrow\rangle_i |\downarrow\rangle_{i+1}$ $\quad$ $|\uparrow\rangle_i |\downarrow\rangle_{i+1}$

$d_{eff}^3/(\lambda/2)^3$ in the 1/10 GHz regime

Conclusions

- OL provide promising systems for the implementation of Quantum Information Processing
  - low decoherence rates
  - large systems
  - controllable, implement Hubbard and Spin Hamiltonians.
- Quantum state engineering with time-dependent potentials: adiabatic ramping, fast oscillatory potential, trains of pulses.
- Detection of strongly correlated phases is possible.
- Some quantum gates have already been implemented experimentally.

→ recent experimental breakthrough: single-site addressing

Thank you very much for your attention!!

1-year post-doctoral position in Madrid available

mirta.rodriguez@iem.cfmac.csic.es